Electronic Supplementary Material (ESI) for Chemical Communications.

Supporting Information

2,6-Dibromogallates as a new building block for controlling π-stacking, network formation and mirror symmetry breaking

Ohjin Kwon[a], Xiaoqian Cai[b], Azhar Saeed,[b] Feng Liu,[b] Silvio Poppe[a] and Carsten Tschierske[a]

[a] Institute of Chemistry, Martin-Luther-University Halle-Wittenberg, Kur-Mother Str. 2, 06120 Halle (Saale), Germany

[b] State Key Laboratory for Mechanical Behaviour of Materials, Shaanxi International Research Center for Soft Matter, Xi'an Jiaotong University, Xi'an 710049, P. R. China

1. Methods

Optical investigation. Phase transitions were observed by polarizing microscopy (Leica DMR XP) in conjunction with a heating stage (FP 82 HT, Mettler) and controller (FP 90, Mettler). Optical investigation was carried out under equilibrium conditions between glass slides which were used without further treatment, sample thickness was ~15 µm. A full wavelength retardation plate was used to determine the sign of birefringence. Optical micrographs were taken using a Leica MC120HD camera.

Calometric investigation. Phase transitions were determined by differential scanning calorimetry (DSC-7 and DSC-8000, Perkin Elmer) at heating/cooling rates of 10 K min^{-1} (peak temperatures). If not otherwise noted transition temperatures and –enthalpies were taken from the second heating and cooling curve.

X-ray diffraction. X-ray investigations (Kristalloflex 760H, Siemens) on powder-like samples were carried out using Ni filtered CuKα radiation (15 to 30 min exposure time). The samples were prepared in the isotropic state on a glass plate and cooled (rate: 5 $K \cdot min^{-1}$) to the measuring temperature. The samples were held on a temperature-controlled heating stage and the diffraction patterns were recorded with a 2D detector (Vantec 500, Bruker); exposure time was 15-20 min. The sample-detector distance for the samples was 9.00 cm for WAXD and 26.80 cm for SAXD measurements. The diffraction patterns obtained were transform to 1D plots using GADDS over the full Chi range.

Synchrotron X-ray diffraction. High-resolution small-angle powder diffraction experiments were recorded on Beamline BL16B1 at Shanghai Synchrotron Radiation Facility, SSRF. Samples were held in evacuated 1 mm capillaries. A Linkam hot stage with a thermal stability within 0.2 ºC was used, with a hole for the capillary drilled through the silver heating block and mica windows attached to it on each side. DECTRIS PILATUS detector was used. *q* calibration and linearization were verified using several orders of layer reflections from silver behenate and a series of *n*-alkanes. The measurement of the positions and intensities of the diffraction peaks is carried out using Galactic PeakSolveTM program, where experimental diffractograms are fitted using Gaussian

shaped peaks. The diffraction peaks are indexed on the basis of their peak positions, and the lattice parameters and the plane/space groups are subsequently determined.

Electron density calculation. The diffraction peaks are indexed on the basis of their peak positions, and the lattice parameters and the space groups are subsequently determined. Once the diffraction intensities are measured and the corresponding space group determined, 3-d electron density maps can be reconstructed, on the basis of the general formula

$$E(xyz) = \Sigma_{hkl} F(hkl) \exp[i2\pi(hx+ky+lz)] \quad \text{(Eqn. 1)}$$

Here $F(hkl)$ is the structure factor of a diffraction peak with index (hkl). It is normally a complex number and the experimentally observed diffraction intensity

$$I(hkl) = K \cdot F(hkl) \cdot F^*(hkl) = K \cdot |F(hkl)|^2 \quad \text{(Eqn. 2)}$$

Here K is a constant related to the sample volume, incident beam intensity etc. In this paper we are only interested in the relative electron densities, hence this constant is simply taken to be 1. Thus, the electron density

$$E(xyz) = \Sigma_{hkl} \text{ sqrt}[I(hkl)] \exp[i2\pi(hx+ky+lz)+\phi_{hkl}] \quad \text{(Eqn. 3)}$$

As the observed diffraction intensity $I(hkl)$ is only related to the amplitude of the structure factor $|F(hkl)|$, the information about the phase of $F(hkl)$, ϕ_{hkl}, cannot be determined directly from experiment. However, the problem is much simplified when the structure of the ordered phase is centrosymmetric, and hence the structure factor $F(hkl)$ is always real and ϕ_{hkl} is either 0 or π. In the case of the centrosymmetric $Ia3d$ phase it is possible for a trial-and-error approach, where candidate electron density maps are reconstructed for all possible phase combinations, and the "correct" phase combination is then selected on the merit of the maps, helped by prior physical and chemical knowledge of the system.

$I23$ phase is non-centrosymmetric so the above approach does not work. In addition, a general (hkl) peak with $h \neq k \neq l$ is only cyclically permutable: it is equivalent to (klh) and (lhk) but not to (hlk), (lkh) and (khl) peaks. Consequently, even though the (hkl) and (lkh) peaks coincide in a powder diffractogram, their intensities and corresponding structure factor phases are different. In order to circumvent these two problems for $I23$ phase we have calculated the diffraction intensities and phases for each observed peak from the Fourier transform of a mathematical model of the phase, where the electron density of a point in the unit cell is chosen to be a higher constant value if it is

within a certain distance to the network segments, and a lower constant value if it is not. The distance is chosen so that the volume ratio of the high electron density regions in the unit cell matches that of the rigid aromatic core in the molecule. After that, we have simply taken from the simulation the intensity ratio of (*hkl*) and (*lkh*) peaks, and the phase angle of each peak, combining them with experimentally observed diffraction intensities to reconstruct the electron density map as shown in Figure 3. More details see ref. [S1]

2. Additional Data

2.1 DSC traces and transition temperatures

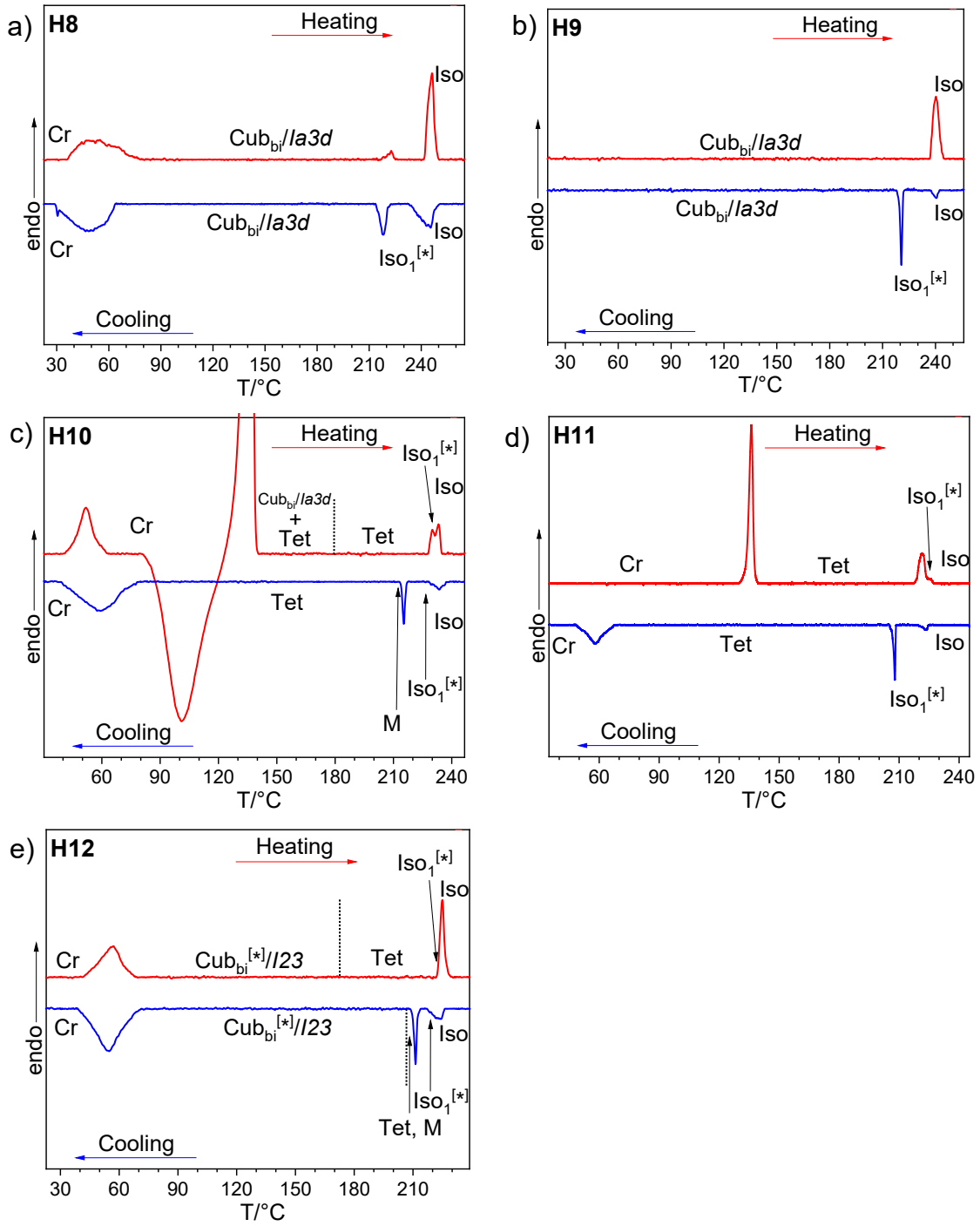

Figure S1. DSC traces (10K·min^{-1}) compounds **H8** – **H12.**

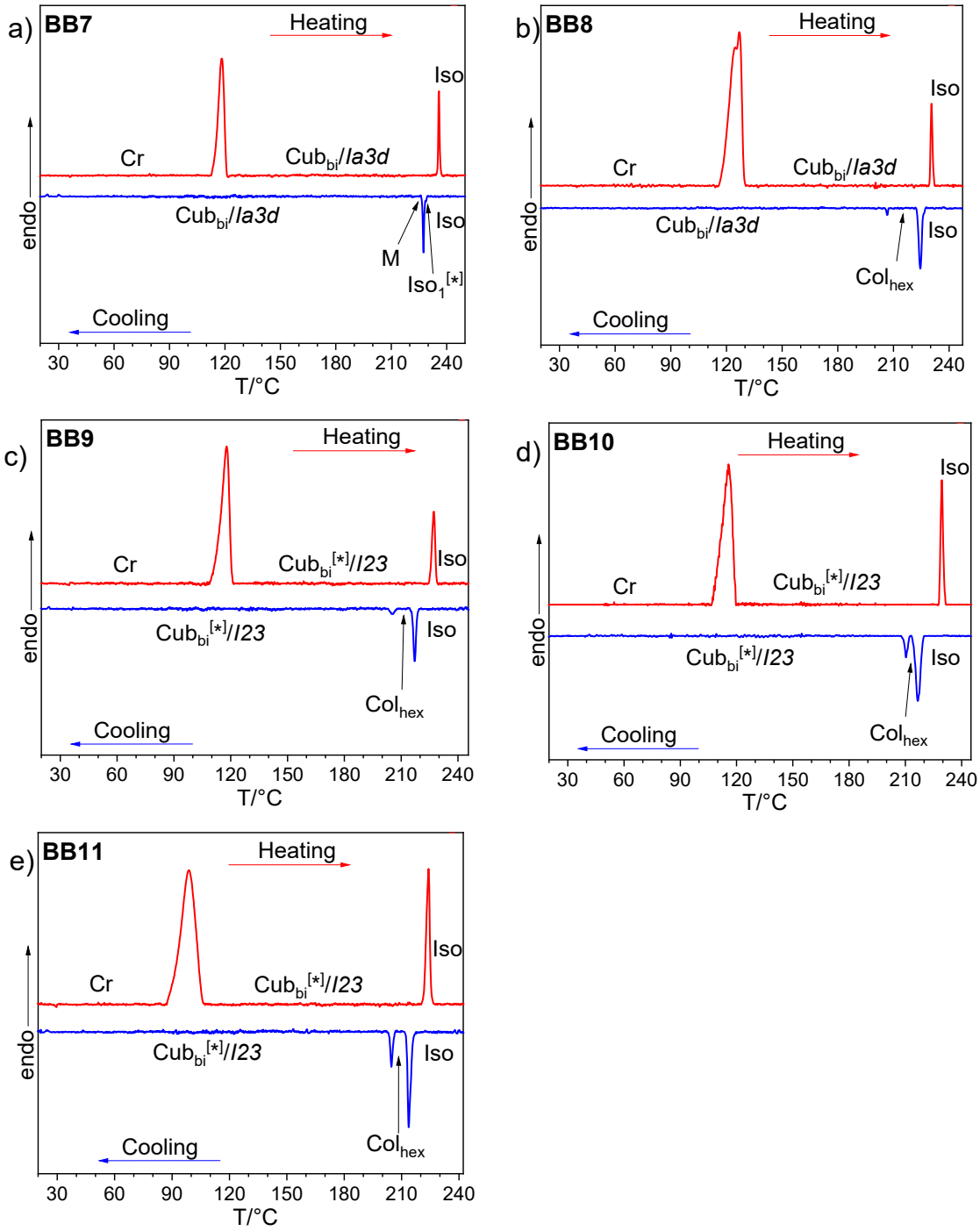

Figure S2. DSC traces (10 K·min^{-1}) compounds **BB7** – **BB11.**

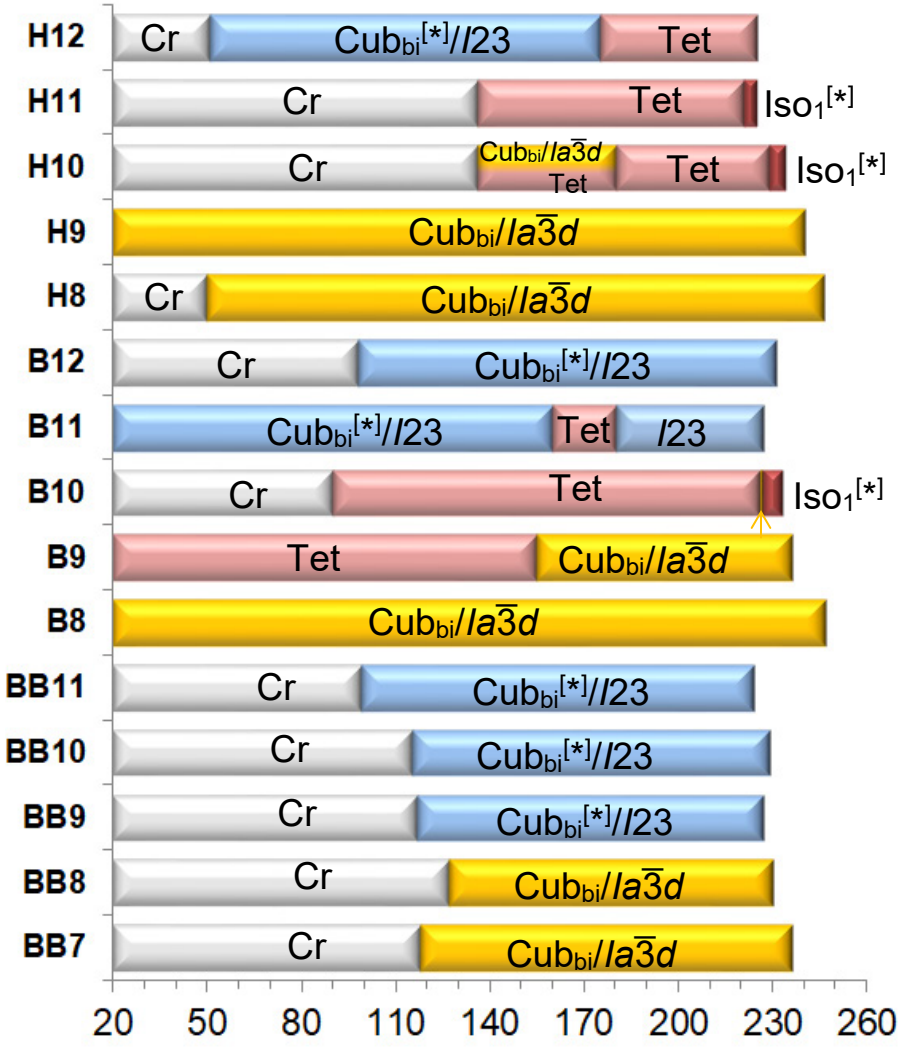

Figure S3. Phases and phase transitions observed in the first heating scan (rate 10 K min^{-1}).

Table S1. Phase transition temperatures (T/°C) and associated enthalpies (ΔH/kJ mol^{-1}) of compounds **H*n*.**

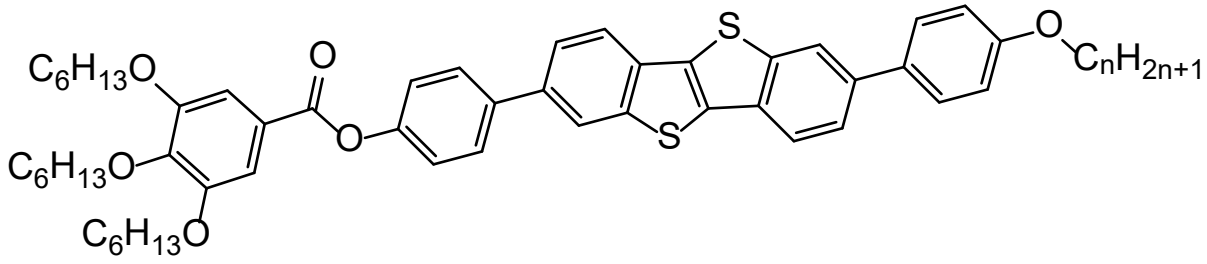

	T/°C [ΔH /kJ·mol^{-1}]
H8	Heating: Cr 50 [2.9] Cub$_{bi}$/*Ia*$\bar{3}$*d* 246 [1.9] Iso Cooling: Iso 245 [-0.4] Iso$_1$[*] 218 [-0.7] Cub$_{bi}$/*Ia*$\bar{3}$*d* 49 [-3.6] Cr
H9	Heating: Cr <20 Cub$_{bi}$/*Ia*$\bar{3}$*d* 240 [1.8] Iso Cooling: Iso 240 [-0.1] Iso$_1$[*] 220 [-0.7] Cub$_{bi}$/*Ia*$\bar{3}$*d* <20 Cr
H10	Heating: Cr 136 [29.9] Cub$_{bi}$/*Ia*$\bar{3}$*d* +Tet 180 Tet 229 Iso$_1$[*] 234 [1.36] Iso Cooling: Iso 234 [-0.2] Iso$_1$[*] 215 Cub$_{bi}$/*Ia*$\bar{3}$*d* 214 M 214 [-0.5][a] Tet 58 [-7.0] Cr
H11	Heating: Cr 136 [4.8] Tet 221 [1.4] Iso$_1$[*] 225 [0.1] Iso Cooling: Iso 224 [-0.2] Iso$_1$[*] 207 [-0.7] M 206 Tet 58 [-5.0] Cr
H12	Heating: Cr 51 [4.5] Cub$_{bi}$[*]/*I*23 175 Tet 223 Iso$_1$[*] 225 [1.7] Iso Cooling: Iso 225 [-0.4] Iso$_1$[*] 212 [-0.7] M 210 Tet 209 Cub$_{bi}$[*]/*I*23 55 [-4.8] Cr

[a] Enthalpy value refers to the transitions Iso$_1$[*] 215 Cub$_{bi}$/*Ia*$\bar{3}$*d* 214 M 214 Tet which cannot be resolved.

Table S2. Phase transition temperatures (T/°C) and associated enthalpies (ΔH/kJ mol^{-1}) of compounds **B*n*** (values from Ref. S8).

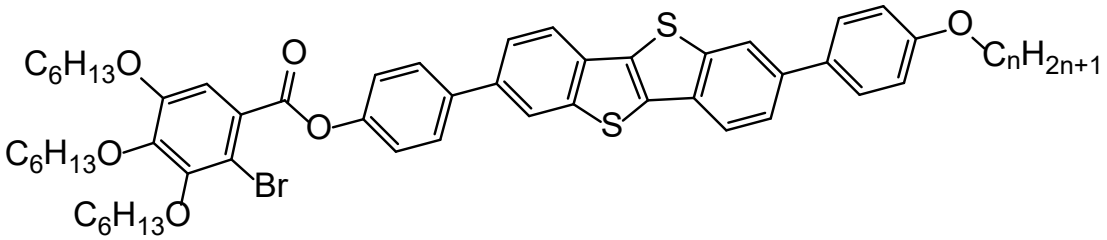

	T/°C [ΔH /kJ·mol^{-1}]
B8	Heating: Cr <20 Cub$_{bi}$/$Ia\bar{3}d$ 247 [2.0] Iso Cooling: Iso 245 [-0.1] Iso$_1$[*] 238 [-1.2] Cub$_{bi}$/$Ia\bar{3}d$ <20 Cr
B9	Heating: Cr <20 Tet 155 [-] Cub$_{bi}$/$Ia\bar{3}d$ 236 [1.7] Iso Cooling: Iso 236 [-0.2] Iso$_1$[*] 221 [-] M 220 [-0.7][b] Cub$_{bi}$/$Ia\bar{3}d$ 150 [-] Tet <20 Cr
B10	Heating: Cr 90 [16.8] Tet 226 [-] Cub$_{bi}$/$Ia\bar{3}d$ 227 [1.7] Iso$_1$[*] 233 Iso Cooling: Iso 233 [-0.1] Iso$_1$[*] 223 M [-] 220 [-0.7][b] Tet <20 Cr
B11	Heating: Cr <20 Cub$_{bi}$[*]/$I23$ 160 [-] Tet 180 [-] Cub$_{bi}$[*]/$I23$ 227 [1.8] Iso Cooling: Iso 220 [-0.1] Iso$_1$[*] 212 M 211 [-0.9][b] Cub$_{bi}$[*]/$I23$ <20 Cr
B12	Heating: Cr 98 [8.0] Cub$_{bi}$[*]/$I23$ 231 [2.5] Iso Cooling: Iso 224 [-0.2] Iso$_1$[*] 219 [-1.7] Cub$_{bi}$[*]/$I23$ <20 Cr

Table S3. Phase transition temperatures (T/°C) and associated enthalpies (ΔH/kJ mol^{-1}) of compounds **BB*n*.**

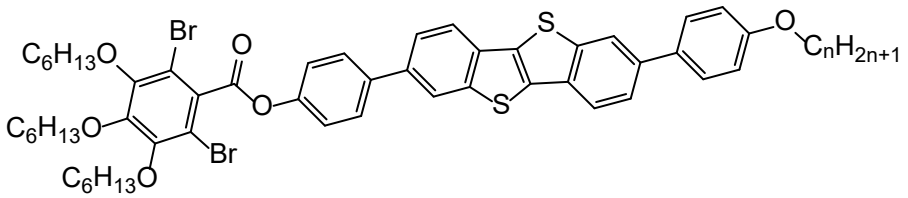

	T/°C [ΔH /kJ·mol^{-1}]
BB7	Heating: Cr 118 [13.5] Cub_{bi}/$Ia\bar{3}d$ 236 [1.9] Iso Cooling: Iso_2 229 Iso_1^* 227 [-1.3] M 226 Cub_{bi}/$Ia\bar{3}d$ <20 Cr
BB8	Heating: Cr 127 [12.7] Cub_{bi}/$Ia\bar{3}d$ 230 [1.4] Iso Cooling: Iso 225 [-0.9] Col_{hex} 208 [1.3] Cub_{bi}/$Ia\bar{3}d$ <20 Cr
BB9	Heating: Cr 117 [12.2] $Cub_{bi}^{[*]}$/$I23$ 227 [2.1] Iso Cooling: Iso 217 [-1.4] Col_{hex} 207 [-0.1] $Cub_{bi}^{[*]}$/$I23$ <20 Cr
BB10	Heating: Cr 115 [9.4] $Cub_{bi}^{[*]}$/$I23$ 229 [2.1] Iso Cooling: Iso 217 [-1.8] Col_{hex} 210 [-0.3] $Cub_{bi}^{[*]}$/$I23$ <20 Cr
BB11	Heating: Cr 99 [11.0] $Cub_{bi}^{[*]}$/$I23$ 224 [2.7] Iso Cooling: Iso_2 214 [-1.6] Col_{hex} 205 [-0.5] $Cub_{bi}^{[*]}$/$I23$ <20 Cr

2.2 Textures

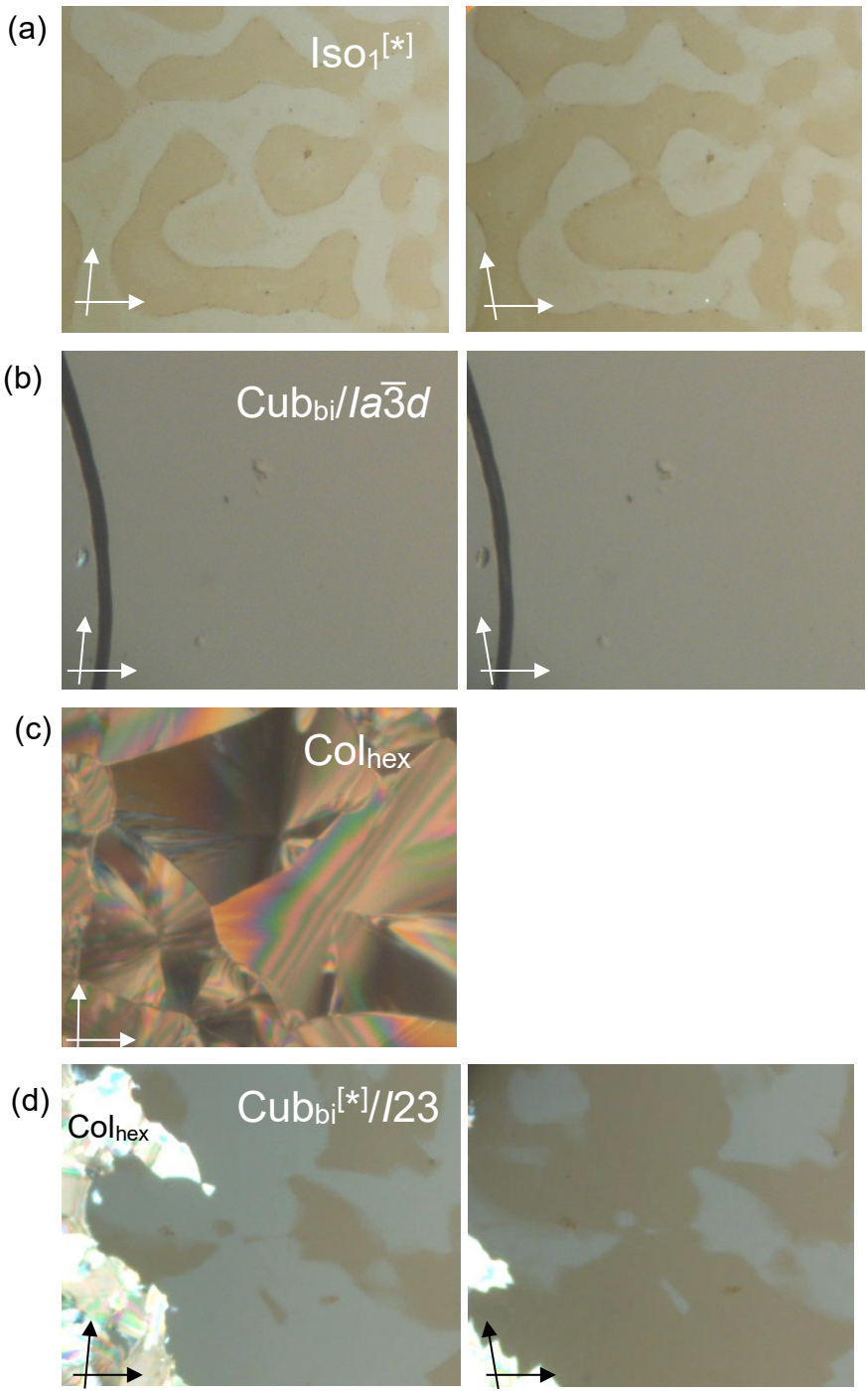

Figure S4. Representative textures on cooling: a) $Iso_1^{[*]}$ of **BB7** at 228 °C; b) $Cub_{bi}/Ia\bar{3}d$ of **BB8** at 200 °C; c) Col_{hex} of **BB9** at 210 °C; d) $Cub_{bi}^{[*]}/I23$ of **BB9** at 205 °C replacing Col_{hex}.

2.3 XRD data and structural data

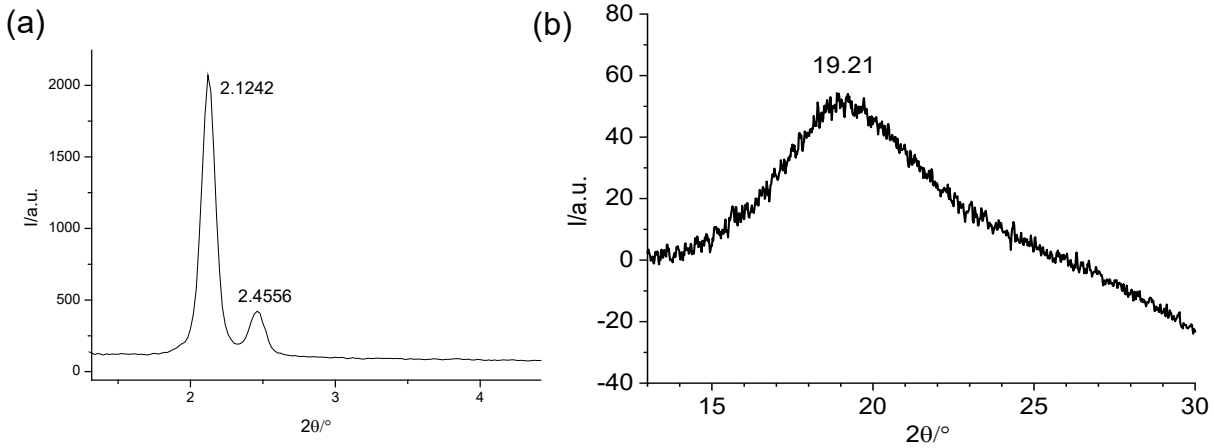

Figure S5. a) SAXS and b) WAXS of **H8** at 180 °C in the $Cub_{bi}/Ia\bar{3}d$ Phase.

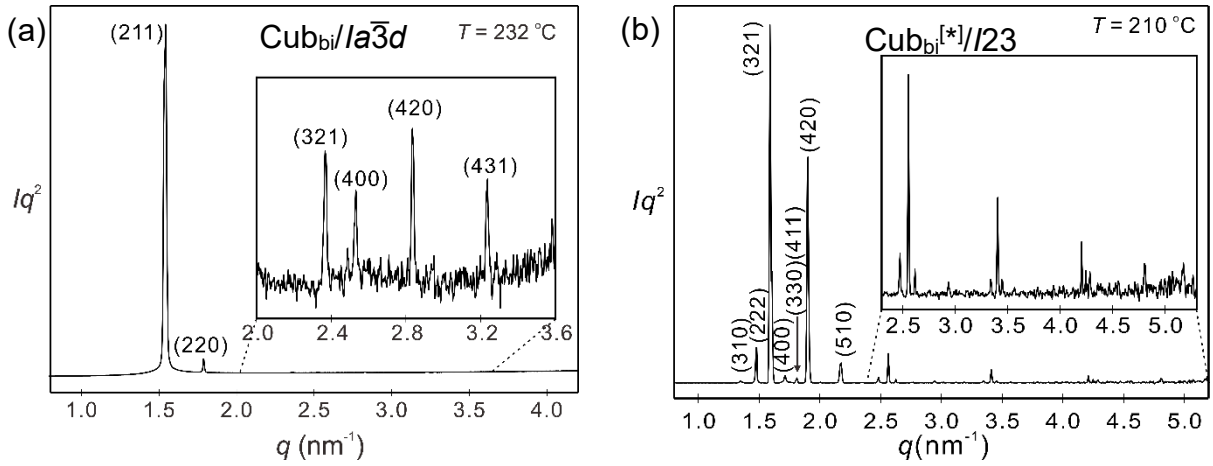

Figure S6. SAXS diffractogram a) of **H10** in the $Cub_{bi}/Ia\bar{3}d$ phase at 232 °C (domain-like pattern) and b) of **H12** in the $Cub_{bi}^{[*]}/I23$ phase at 210 ºC (domain-like pattern).

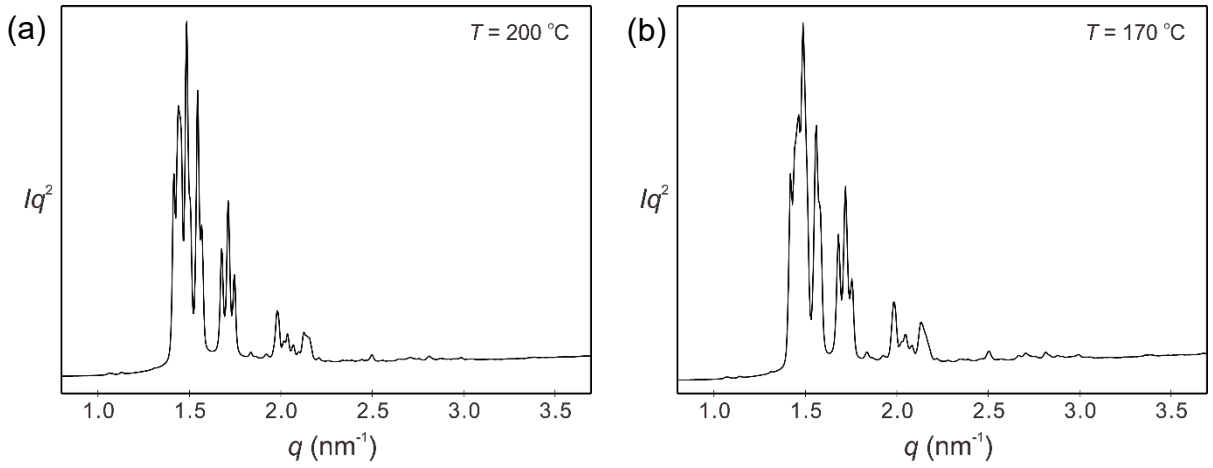

Figure S7. SAXS diffractogram of Tet phase of a) **H10** at 200 °C and b) **H12** at 170 ºC.

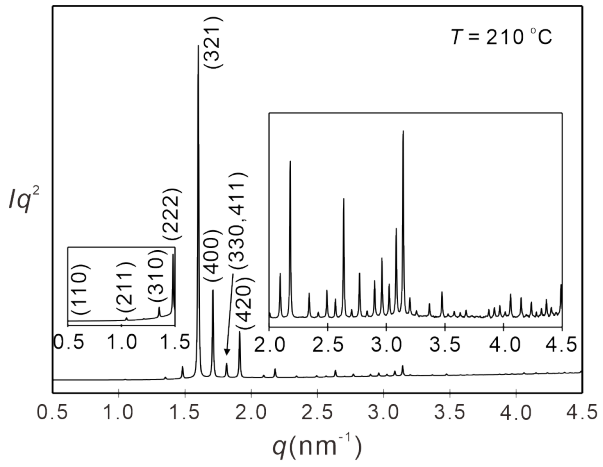

Figure S8. SAXS diffractogram of $Cub_{bi}^{[*]}/I23$ phase of **BB11** at 210 ºC on heating.

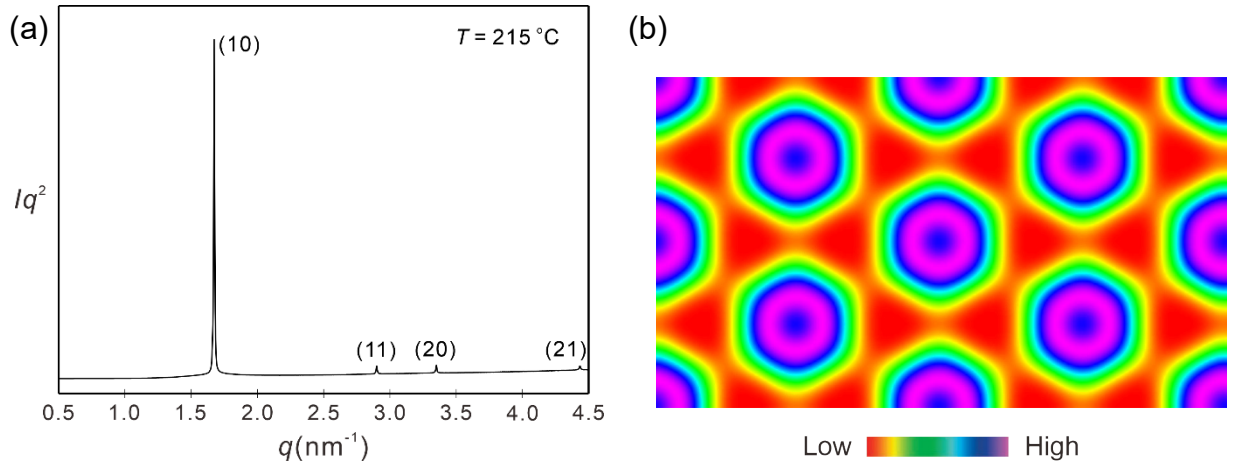

Figure S9. BB11: a) SAXS diffractogram of Col_{hex}/*p6mm* phase at 215 ºC on cooling and b) reconstructed electron density map of Col_{hex}/*p6mm* phase.

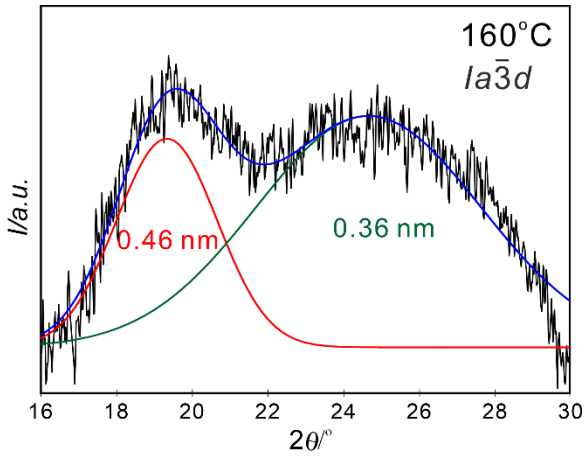

Figure S10. WAXS pattern of compound **BB7** in the Cub_{bi}/*Ia*$\bar{3}$*d* phase at 160 °C. Blue line represents the fitted curve and red/green lines are the resolved peaks. The WAXS were performed by Kristalloflex 760H with CuKα radiation.

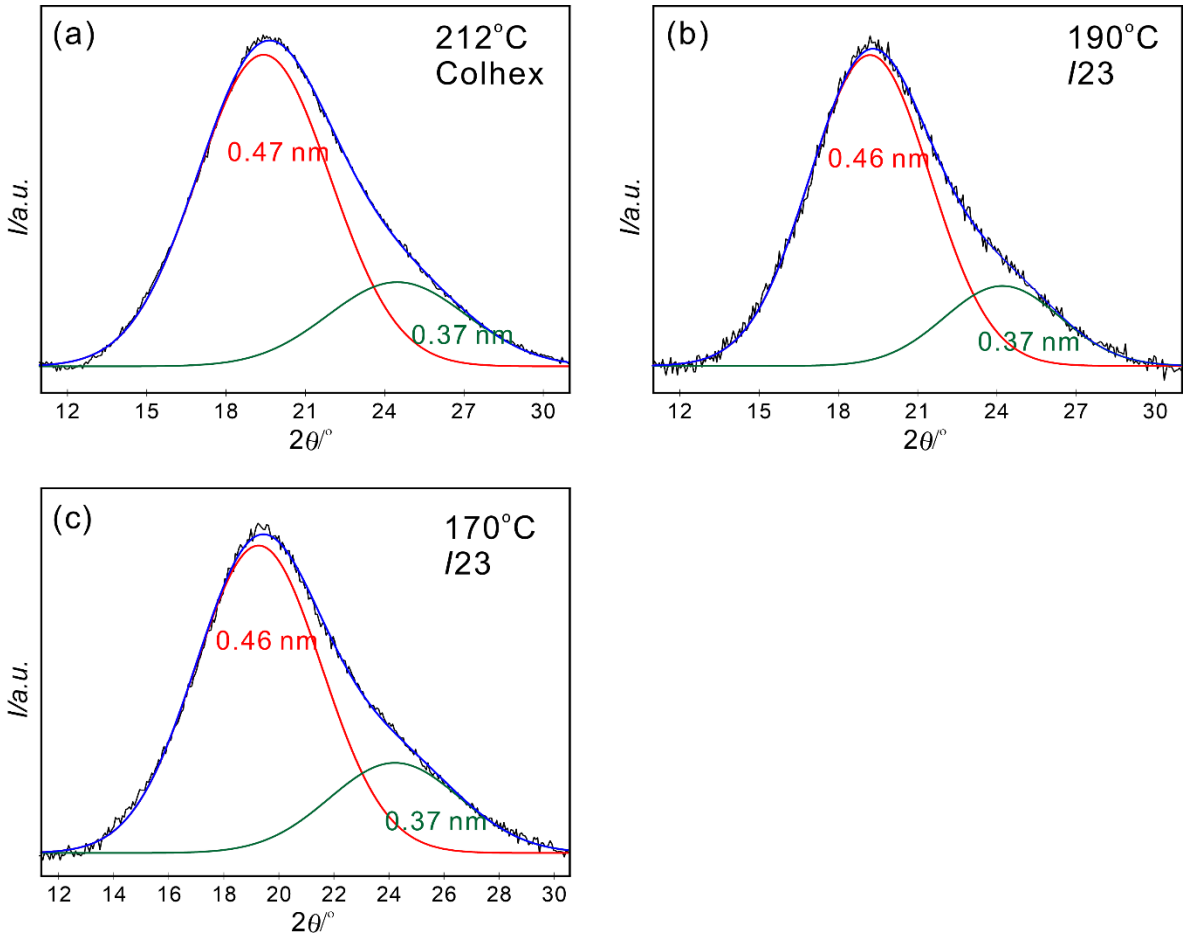

Figure S11. WAXS diffractograms of **BB11** on cooling: (a) Col_{hex}/*p6mm* phase at 212 °C; (b) $Cub_{bi}^{[*]}$/*I*23 phase at 190 °C; (c) $Cub_{bi}^{[*]}$/*I*23 phase at 170 °C. Blue lines represent the fitted curves and red/green lines are the resolved peaks. The Temperature dependence investigations of WAXS were performed by Anton Paar SAXSpoint 2.0 with CuKα radiation.

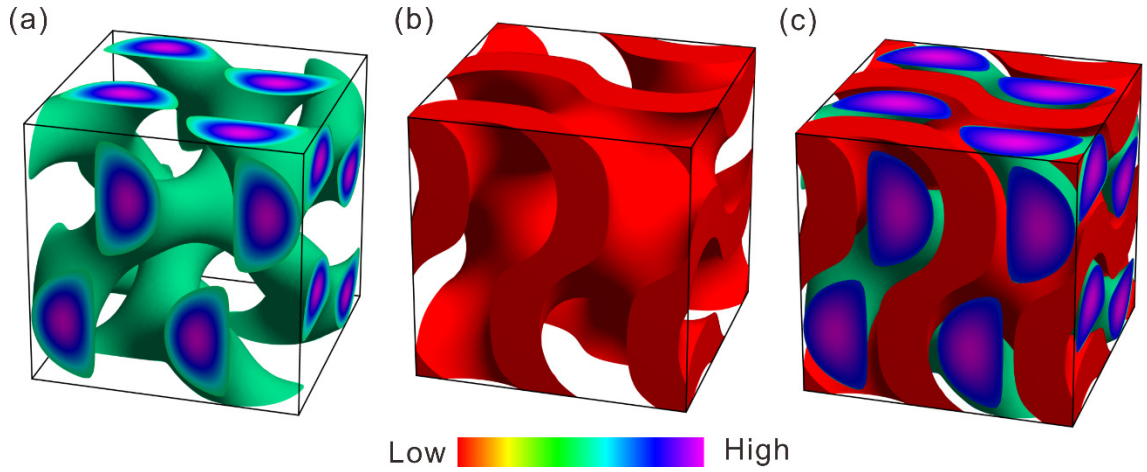

Figure S12. Reconstructed electron density maps of $Cub_{bi}/Ia\bar{3}d$ phase of **BB7**: (a) high electron density regions involving the aromatic cores and the glycerol groups; (b) low electron density regions containing the alkyl chains; (c) electron density maps of $Cub_{bi}/Ia\bar{3}d$ phase.

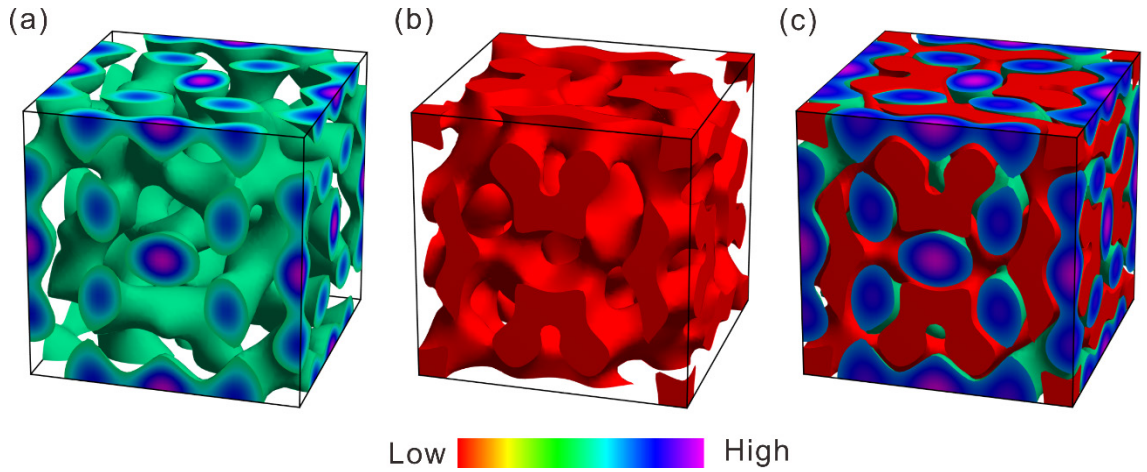

Figure S13. Reconstructed electron density maps of $Cub_{bi}^{[*]}/I23$ phase of **BB9**: (a) high electron density regions involving the aromatic cores and the glycerol groups; (b) low electron density regions containing the alkyl chains; (c) electron density maps of $Cub_{bi}^{[*]}/I23$ phase.

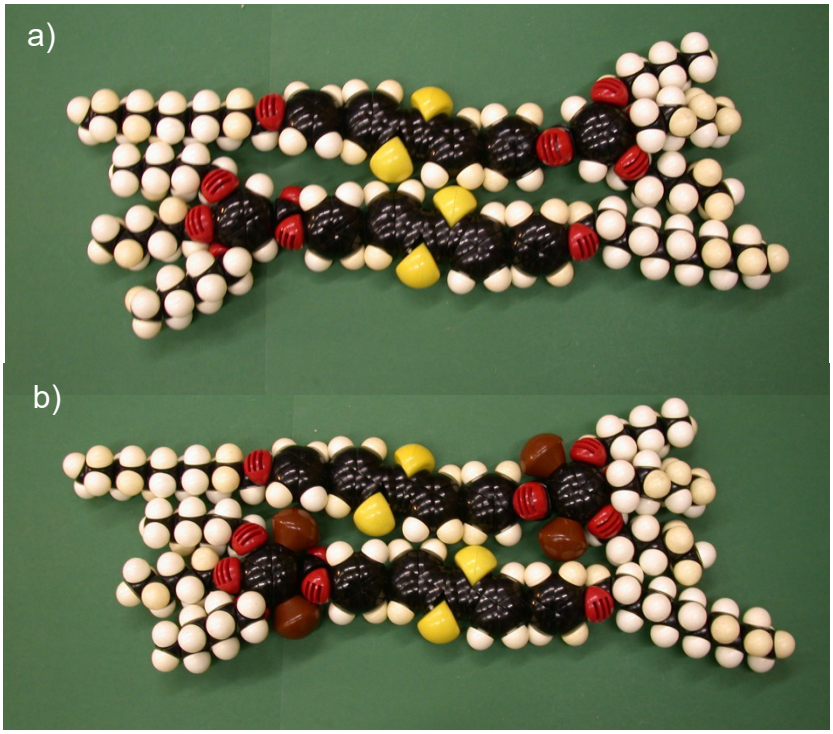

Figure S14. Space filling CPK models of compounds a) **H10** and b) **BB10** (L_{mol} = 4.8 nm). In b) the bromines fill the void space around the COO groups.

Table S4. Experimental and calculated *d*-spacing of the observed SAXS and WAXS reflection of the Cub/$Ia\bar{3}d$ phase in **H8** at 180 °C.

2θ	Theta	d – value (nm)	d_{calc} (nm)	(*hkl*)	Δ
2.124	1.062	4.159	4.159	211	0.00
2.456	1.228	3.598	3.602	220	0.00
19.213	9.607	0.462		diff	
a_{cub} = 10.19 nm					

Table S5. Experimental, calculated *d*-spacings and relative integrated intensities of the Cub/$Ia\bar{3}d$ phase in **H10** at 232ºC. All intensities values are Lorentz and multiplicity corrected (domain-like pattern).

(*hkl*)	$d_{obs.}$ - spacings (nm)	$d_{cal.}$ - spacings (nm)	*intensity*
(211)	4.06	4.06	100.00
(220)	3.50	3.52	6.68
(321)	2.65	2.66	0.12
(400)	2.48	2.49	0.43
(420)	2.22	2.22	0.24
(431)	1.94	1.95	0.17
a_{cub} = 9.95 nm			

Table S6. Experimental and calculated *d*-spacings of the $Cub_{bi}^{[*]}/I23$ phase in **H12** at 210ºC (domain-like pattern).

(*hkl*)	$d_{obs.}$ - spacings (nm)	$d_{cal.}$ - spacings (nm)
(310)	4.68	4.69
(222)	4.28	4.28
(321)	3.96	3.96
(400)	3.68	3.71
(330)	3.48	3.50
(411)		
(420)	3.39	3.32
(431)	2.89	2.91
(510)		
(433)	2.54	2.54
(530)		
(442)	2.45	2.47
(600)		
(532)	2.40	2.41
(611)		
(444)	2.14	2.14
(651)	1.88	1.88
(732)		
(800)	1.84	1.85
(554)	1.82	1.83
(741)		
(811)		
a_{cub} = 14.83 nm		

Table S7. Experimental and calculated *d*-spacings, relative integrated intensities, and phases used in the reconstruction of electron densities for the $\mathrm{Cub}/Ia\bar{3}d$ phase in **BB7** at 170ºC. All intensities values are Lorentz and multiplicity corrected.

(*hkl*)	$d_{obs.}$ - spacings (nm)	$d_{cal.}$ - spacings (nm)	*intensity*	*phase*
(211)	4.00	4.00	100.0	π
(220)	3.46	3.46	41.7	π
(321)	2.61	2.62	0.5	/
(400)	2.44	2.45	0.9	/
(420)	2.19	2.19	2.1	/
(332)	2.09	2.09	4.7	/
(422)	2.00	2.00	0.9	/
(431)	1.92	1.92	0.02	/
(440)	1.73	1.73	0.8	/
(611)	1.59	1.59	0.1	/
(532)			0.05	/
(541)	1.51	1.51	0.09	/
(631)	1.44	1.44	0.08	/
(444)	1.41	1.41	2.0	/
(543)	1.38	1.39	1.0	/
(721)	1.33	1.33	0.7	/
(633)			1.5	/
(552)			1.5	/
(642)	1.30	1.31	0.03	/
(800)	1.23	1.23	0.6	/
a_{cub} = 9.80 nm				

Table S8. Experimental and calculated *d*-spacings, relative integrated intensities, and phases used in the reconstruction of electron densities for the $Cub_{bi}^{[*]}/I23$ phase in **BB9** at 170ºC. All intensities values are Lorentz and multiplicity corrected.

(*hkl*)	$d_{obs.}$ - spacings (nm)	$d_{cal.}$ - spacings (nm)	*intensity*	*phase*
(110)	10.33	10.41	0.02	/
(211)	6.01	6.01	0.22	-0.97π
(220)	5.20	5.20	0.14	/
(301)	4.65	4.65	1.49	0
(222)	4.25	4.25	11.77	-0.24π
(321)	3.93	3.93	36.60	-0.91π
(312)			81.09	-0.59π
(400)	3.69	3.68	100.0	0
(411)	3.47	3.47	1.99	-0.81π
(330)			2.18	0
(420)	3.28	3.29	33.26	0
(332)	3.14		0.19	/
(422)	3.01	3.00	1.12	/
(510)	2.89	2.89	0.93	/
(431)			0.47	/
(521)	2.69	2.69	0.31	/
(440)	2.60	2.60	0.10	/
(530)	2.52	2.52	0.40	/
(442)	2.45	2.45	0.60	/
(611)	2.39	2.39	0.60	/
(532)			0.30	/
(620)	2.33	2.33	0.10	/
(541)	2.27	2.27	0.60	/

(622)	2.22	2.22	0.20	/
(631)	2.17	2.17	0.50	/
(444)	2.13	2.12	4.63	/
(710)	2.08	2.08	0.09	/
(550)			0.21	/
(543)			0.04	/
(640)	2.04	2.04	1.82	/
(721)	2.00	2.00	0.21	/
(633)			0.40	/
(552)			0.40	/
(642)	1.96	1.97	0.23	/
(730)	1.93	1.93	0.22	/
(732)	1.87	1.87	0.03	/
(651)			0.03	/
(811)	1.81	1.81	0.05	/
(741)			0.03	/
(554)			0.05	/
(820)	1.79	1.79	0.01	/
(644)			0.01	/
(653)	1.75	1.76	0.05	/
(822)	1.73	1.73	0.02	/
(660)			0.04	/
(750)	1.71	1.71	0.04	/
(831)			0.02	/
(840)	1.65	1.65	0.09	/
(910)	1.62	1.63	0.08	/
(833)			0.08	/

(842)	1.60	1.61	0.20	/
(921)	1.58	1.59	0.02	/
(761)			0.02	/
(655)			0.03	/
(664)	1.57		0.20	/
(930)	1.55	1.55	0.07	/
(851)			0.04	/
(754)			0.04	/
(932)	1.52	1.52	0.10	/
(763)			0.10	/
(844)	1.50	1.50	0.10	/
(941)	1.48	1.49	0.02	/
(853)			0.02	/
(770)			0.07	/
(10 1 1)	1.46	1.46	0.07	/
(772)			0.07	/
(10 2 0)	1.44	1.44	0.10	/
(862)			0.05	/
(950)	1.43	1.43	0.20	/
(10 2 2)	1.41	1.42	0.02	/
(666)			0.07	/
(10 3 1)	1.40	1.40	0.05	/
(952)			0.05	/
(765)			0.05	/
(871)	1.38	1.38	0.04	/
(855)			0.08	/
(774)			0.08	/

(10 4 0)	1.36	1.37	0.10	/
(864)			0.07	/
(10 3 3)	1.35	1.36	0.2	/
(961)			0.1	/
(10 4 2)	1.34	1.34	0.2	/
(11 1 0)	1.33	1.33	0.03	/
(954)			0.02	/
(873)			0.02	/
a_{cub} = 14.72 nm				

Table S9. Experimental and calculated *d*-spacings, relative integrated intensities, and phases used in the reconstruction of electron densities for the $Cub_{bi}^{[*]}/I23$ phase in **BB11** at 210ºC. All intensities values are Lorentz and multiplicity corrected.

(*hkl*)	$d_{obs.}$ – spacings (nm)	$d_{cal.}$ – spacings (nm)	*intensity*	*phase*
(110)	10.38	10.39	0.01	/
(211)	6.00	6.00	0.15	-0.97π
(220)	5.19	5.19	0.07	/
(310)	4.65	4.65	1.12	0
(222)	4.24	4.24	9.38	-0.24π
(321)	3.93	3.93	28.96	-0.91π
(312)			61.16	-0.59π
(400)	3.67	3.67	100.00	0
(330)	3.46	3.46	3.11	0
(411)			2.84	-0.81π
(420)	3.29	3.29	12.77	0
(332)	3.13	3.13	0.07	/
(422)	3.00	3.00	0.67	/
(431)	2.88	2.88	0.61	/
(510)			1.21	/
(521)	2.68	2.68	0.18	/
(440)	2.60	2.60	0.14	/
(433)	2.52	2.52	0.20	/
(530)			0.20	/
(442)	2.45	2.45	0.13	/
(600)			0.53	/
(532)	2.38	2.38	0.43	/
(611)			0.86	/

(620)	2.32	2.32	0.11	/
(541)	2.27	2.27	0.35	/
(622)	2.22	2.22	0.09	/
(631)	2.17	2.17	0.26	/
(444)	2.12	2.12	2.44	/
(543)	2.08	2.08	0.08	/
(550)			0.31	/
(710)			0.16	/
(640)	2.04	2.04	1.30	/
(552)	2.00	2.00	0.95	/
(633)			0.95	/
(721)			0.48	/
(642)	1.96	1.96	0.12	/
(730)	1.93	1.93	0.09	/
(651)	1.87	1.87	0.05	/
(732)			0.05	/
(554)	1.81	1.81	0.13	/
(741)			0.06	/
(811)			0.13	
(644)	1.78	1.78	0.02	/
(820)			0.02	/
(653)	1.76	1.76	0.05	/
(660)	1.73	1.73	0.06	/
(822)			0.03	/
(743)	1.71	1.71	0.02	/
(750)			0.04	/
(831)			0.02	

(833)	1.62	1.62	0.05	/
(910)			0.05	/
(842)	1.60	1.60	0.07	/
(655)	1.58	1.58	0.06	/
(761)			0.03	/
(921)			0.03	/
(664)	1.57	1.57	0.07	/
(754)	1.55	1.55	0.06	/
(851)			0.06	/
(930)			0.12	/
(763)	1.51	1.52	0.07	/
(932)			0.07	/
(770)	1.48	1.48	0.13	/
(853)			0.03	/
(941)			0.03	/
(860)	1.47	1.47	0.03	/
(10 0 0)			0.13	/
(772)	1.45	1.45	0.05	/
(10 1 1)			0.05	/
(862)	1.44	1.44	0.06	/
(10 2 0)			0.12	/
(943)	1.43	1.43	0.04	/
(950)			0.07	/
(666)	1.41	1.41	0.10	/
(10 2 2)			0.03	/
(765)	1.40	1.40	0.07	/
(952)			0.07	/

(10 3 1)			0.07	/
(774)	1.37	1.38	0.09	/
(855)			0.09	/
(871)			0.05	/
(864)	1.36	1.36	0.04	/
(10 4 0)			0.08	/
(961)	1.35	1.35	0.07	/
(10 3 3)			0.14	/
(10 4 2)	1.34	1.34	0.05	/
(873)	1.33	1.33	0.02	/
(954)			0.02	/
(11 1 0)			0.04	/
(963)	1.31	1.31	0.03	/
(10 5 1)			0.03	/
(11 2 1)			0.03	/
a_{cub} = 14.69 nm				

Table 10. Experimental and calculated *d*-spacings, relative integrated intensities, and phases used in the reconstruction of electron densities for the Col_{hex}/*p6mm* phase in **BB11** at 235 ºC. All intensities values are Lorentz and multiplicity corrected.

(*hk*)	$d_{obs.}$ – spacings (nm)	$d_{cal.}$ – spacings (nm)	*intensity*	*phase*
(10)	3.75	3.75	100.0	0
(11)	2.17	2.17	2.8	π
(20)	1.88	1.88	2.7	π
(21)	1.42	1.42	0.9	π
a_{hex}= 4.33 nm				

Table S11. Lattice parameters and structural data of the mesophases of the investigated compounds.[a]

Comp.	Phase	T/°C	a,c/ nm	V_{cell}/ nm^3	V_{mol}/ nm^3	n_{cell}	d_{net}	L_{net}	n_{raft}	Φ/°
H8	$Cub_{bi}/Ia\bar{3}d$	180	10.19	1058	1.308	723	4.41	86.46	3.76	8.79
H10	$Cub_{bi}/Ia\bar{3}d$	232	9.95	985	1.357	648	4.31	84.43	3.45	9.01
H10	Tet	200	17.72 15.84	4974	1.357	3273	-	-	-	-
H12	$Cub_{bi}^{[*]}/I23$	220	14.83	3262	1.407	2070	-	306.68	3.04	9.42
B8	$Cub_{bi}/Ia\bar{3}d$	200	10	1000	1.334	670	4.33	84.85	3.55	8.96
B9	$Cub_{bi}/Ia\bar{3}d$	180	9.98	994	1.358	653	4.32	84.68	3.47	8.98
B9	Tet	170	17.72 22.52	7071	1.358	4649	-	-	-	-
B10	$Cub_{bi}/Ia\bar{3}d$	250	9.77	933	1.383	602	4.23	82.90	3.27	9.17
B10	Tet	130	17.85 20.15	6420	1.383	4145	-	-	-	-
B11	Tet	170	17.78 20.15	6370	1.408	4040	-	-	-	-
B11	$Cub_{bi}^{[*]}/I23$	200	14.87	3288	1.408	2085	-	307.51	3.05	9.39
BB7	$Cub_{bi}/Ia\bar{3}d$	170	9.80	941	1.335	630	4.24	83.15	3.41	9.14
BB9	$Cub_{bi}^{[*]}/I23$	170	14.72	3190	1.385	2057	-	304.41	3.04	9.49
BB11	$Cub_{bi}^{[*]}/I23$	210	14.69	3170	1.434	1974	-	303.79	2.92	9.51
BB11	$Col_{hex}/p6mm$	235	4.33	7.307	1.434	4.55	-	-	4.55	-

[a] Abbreviations: $V_{cell} = a_{cub}^3$ = volume of the unit cell; for the tetragonal phase $V_{cell} = a^2$ x c, for Col_{hex} phases a height h of 0.45 nm is assumed: $V_{cell} = h(\sqrt{3}a_{hex}^2/2)$; V_{mol} = volume of the molecule as calculated with the crystal volume increments of Immirzi[S2] n_{cell} = number of molecules per unit cell, calculated according to 0.893 V_{cell}/V_{mol}, where the factor 0.893 is a correction for the different packing density in the crystalline and the LC state; d_{net} = lateral distance between the nets in the $Ia\bar{3}d$ phase, calculated according to: $d_{net} = \sqrt{3}(a_{cub}/4)$, L_{net} = total length of the netwoks per unit cell ($L_{net} = 8.485a_{Ia3d}$ and $L_{net} = 20.68a_{I23}$, respectively;[S1] n_{raft} = number molecules organized in each 0.45 nm tick raft of the networks or columns, calculated according to $n_{raft} = n_{cell}/(L_{net}/0.45)$; for Col_{hex}: $n_{raft} = n_{cell}$; Φ = twist angle between adjacent molecules (or rafts of molecules) in the networks of the $Ia\bar{3}d$ -phases; $\Phi(Ia\bar{3}d) = 70.5°/[0.354a_{cub}/0.45nm]$, $\Phi(I23) = 90°/[0.290a_{cub}/0.45nm]$;[S1] for XRD data, see Tables S4-S10.

2.4 Additional discussions

As noted in the main text the 2,6-difluorination at the apex instead of the trisubstituted end leads to a significant decrease of the mesophase stability and removal of the Cub_{bi} phase, even if the much smaller fluorine is used, see Scheme S1.

.

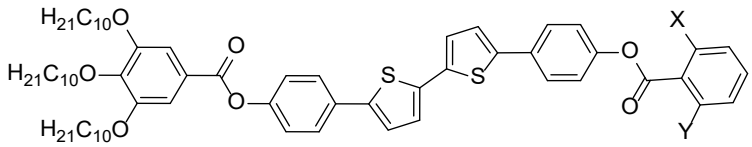

1H (X = Y = H): Cr 114 Cub_{bi}/*Ia*$\bar{3}$*d* 162 Iso (°C)
1F: (X = H; Y = F): Cr 92 Cub_{bi}/*Ia*$\bar{3}$*d* 143 Iso (°C)
1F2 (X = Y = F): Cr 118 SmC 112 Iso (°C)

Scheme S1. Effect of inside directed fluorination of the bithiophene **1H** on the mesophases stability. The comparison of the non-fluorinated bithiophene **1H** with the fluorinated compounds **1F** and **1F2** demonstrates the strong mesophase destabilizing and Cub_{bi} phase removing effect of this substitution pattern.[S3]

3. Synthesis and analytical data

3.1 Synthesis of H8-H12

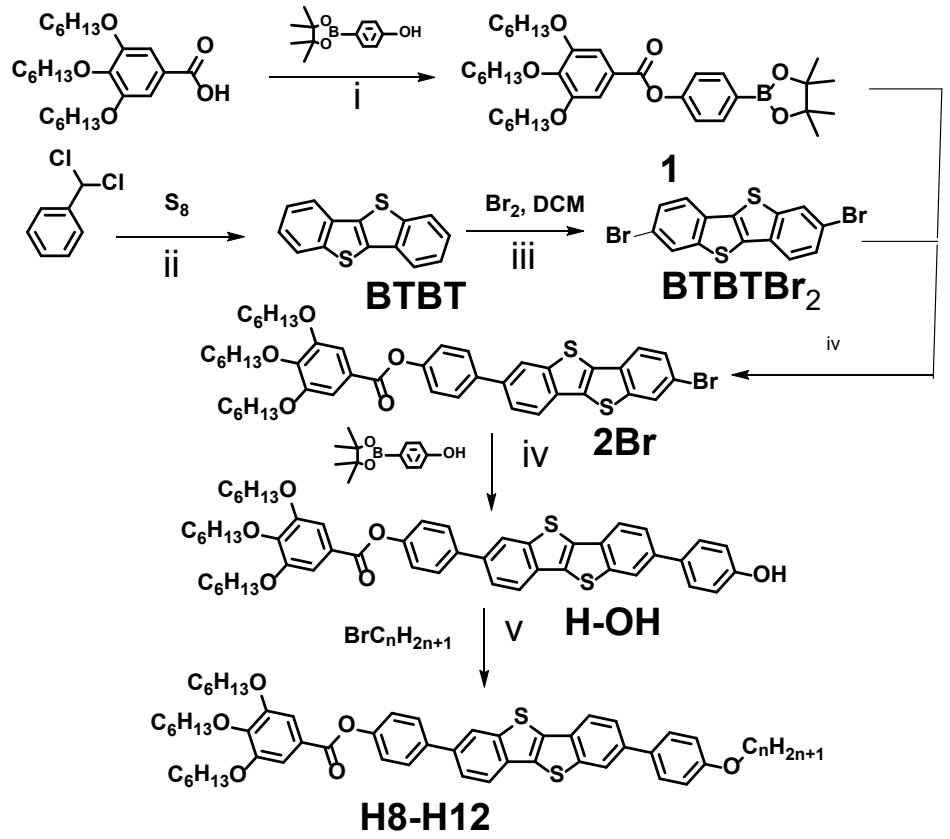

Scheme S2. Synthesis of compounds **H8**-**H12**. Reagents and conditions: (i) $SOCl_2$, dry pyridine, RT; (ii) 260 °C; (iii) DCM, RT; (iv) THF, sat. $NaHCO_3$ solution, $[Pd(PPh_3)_4]$, reflux; (v) dry 2-butanone, K_2CO_3; TBAI; reflux.

3.1.2 Intermediates

4-(3,4,5-Tri-n-hexyloxybenzoyloxy)phenylboronic acid pinacol ester (1) was prepared according to reported standard procedures [S4 ,S5]

2,7- Dibromo [1]benzothieno[3,2-b]benzothiophene (BTBTBr2); BTBT (5.00 g, 0.0208 mol) was dissolved in DCM (300 ml). Bromine (7.20 g, 0.0451 mol) with DCM was prepared in a dropping funnel and added dropwise to the solution. The mixture was stirred for 48h at RT. The

reaction was quenched by adding $Na_2S_2O_3$ solution. The crude product was filtered and washed with H_2O. Then, It was purified by extraction in a Soxhlet apparatus using DCM as solvent. The final product was recrystallized in the cold DCM; [S6] yield 4.1 g (0.0095 mol, 46%); colorless solid; m.p. 299 °C; ^{1}H NMR (400 MHz, $CDCl_3$) δ 8.06 (d, *J* = 1.7 Hz, 2H), 7.73 (d, *J* = 8.5 Hz, 2H), 7.58 (dd, *J* = 8.5, 1.7 Hz, 2H).

2-[4-(3,4,5-Tri-n-hexyloxybenzoyloxy)phenyl]-7-bromo-[1]benzothieno[3,2-b]benzothiophene (2Br): Suzuki coupling reaction was used. [S7] In two-neck flask, **1** (2.19 g, 3.50 mmol) **BTBTBr2** (1.59 g, 4.00 mmol), THF (50 ml), toluene (100 ml) and saturated $NaHCO_3$ solution (70 ml) were prepared, and degassed with argon for 15 minutes. After purging, [$Pd(PPh_3)_4$] (0.1 g, 0.0865 mmol) was added. The solution was refluxed for 6 hours. When the mixture was cooled down, the organic phase was extracted with Toluene. Then, it was dried over Na_2SO_4. After it was concentrated in vacuum, it was purified by column chromatography (eluent: $CHCl_3$/n-hexane 2/1) [S5]; yield 1.20 g (1.47 mmol, 42 %) colorless solid; heating: Cr 128 SmA 150 Iso (°C); cooling: Iso 141 SmA 88 Cr (°C); ^{1}H NMR (500 MHz, $CDCl_3$) δ 8.10 (dd, *J* = 26.4, 1.2 Hz, 2H, BTBT-H), 7.94 (tdd, *J* = 28.3, 8.1, 0.6 Hz, 2H, BTBT-H), 7.77 – 7.69 (m, 3H, BTBT-H + Ar-H), 7.58 (dd, *J* = 8.4, 1.7 Hz, 1H, BTBT-H), 7.44 (s, 2H, Ar-H), 7.34 – 7.31 (m, 2H, Ar-H), 4.12 – 4.05 (m, 6H, OCH_2CH_2), 1.89 – 1.75 (m, 6H, OCH_2CH_2), 1.56 – 1.48 (m, 6H, CH_2), 1.41 – 1.32 (m, 12H, CH_2), 0.95 – 0.89 (m, 9H, CH_3).

2-[4-(3,4,5-Tri-n-hexyloxybenzoyloxy)phenyl]-7-(4-hydroxyphenyl)-[1]benzothieno[3,2-b]benzothiophene (H-OH): The same procedure for **2Br** was used. **2Br** (1.20 g, 1.47 mmol), 4-hydroxyphenylboronic acid pinacol ester (0.33 g, 1.50 mmol), THF (100 ml) and saturated $NaHCO_3$ solution (50 ml), column chromatography (eluent: $CHCl_3$/MeOH 19/1); yield 0.65 g (0.785 mmol, 53 %); colorless solid; heating: Cr 215 SmA 238 Iso (°C); cooling: Iso 236 SmA 179 Cr (°C); ^{1}H NMR (400 MHz, $CDCl_3$) δ 8.04 (dd, *J* = 38.3, 0.4 Hz, 2H, BTBT-H), 7.96 – 7.84 (m, 2H, BTBT-H), 7.73 (d, *J* = 8.6 Hz, 2H, Ar-H), 7.70 – 7.58 (m, 2H, BTBT-H), 7.51 (d, *J* = 10.0 Hz, 1H, BTBT-H), 7.46 (s, 2H, Ar-H), 7.32 (d, *J* = 8.6 Hz, 2H, Ar-H), 6.89 (d, *J* = 8.4 Hz, 2H, Ar-H), 5.14 (s, 1H, Ar-OH), 4.14 – 4.01 (m, 6H, OCH_2CH_2), 1.91 – 1.73 (m, 6H, OCH_2CH_2), 1.63 – 1.44 (m, 6H, CH_2), 1.43 – 1.29 (m, 12H, CH_2), 0.97 – 0.87 (m, 9H, CH_3).

3.1.3 Compounds H8 – H12

Williamson ether synthesis was used for the final step. **H-OH** (120 mg, 0.1449 mmol), K_2CO_3 (200 mg, 1.449 mmol), TBAI (20 mg, 0.0620 mmol), 1-bromoalkane (0.4346 mmol) are prepared in butanone (50 ml). The solution is refluxed for 5 hours. Butanone was removed via rotary evaporator and the crude product was purified via liquid column chromatography with (chloroform/n-hexane 2/1). Then, recrystallization from THF/EtOH is repeated.

2-[4-(3,4,5-Tri-n-hexyloxybenzoyloxy)phenyl]-7-(4-octyloxyphenyl)-[1]benzothieno[3,2-b]benzothiophene (H8): H-OH (100 mg, 0.121 mmol), K_2CO_3 (200 mg, 1.447 mmol), TBAI (20 mg, 0.0541 mmol), 1-bromooctane (70 mg, 0.362 mmol) and butanone (50 ml); yield 30 mg (0.0319 mmol, 26%); colorless solid; M = 941.33 g mol^{-1}; ^{1}H NMR (500 MHz, $CDCl_3$) δ 8.12 (dd, *J* = 22.5, 0.9 Hz, 2H, BTBT-H), 7.94 (dd, *J* = 12.0, 8.2 Hz, 2H, BTBT-H), 7.75 (d, *J* = 8.6 Hz, 2H, Ar-H), 7.69 (ddd, *J* = 16.7, 8.3, 1.4 Hz, 2H, BTBT-H), 7.62 (d, *J* = 8.7 Hz, 2H, Ar-H), 7.45 (s, 2H, Ar-H), 7.33 (d, *J* = 8.6 Hz, 2H, Ar-H), 7.02 (d, *J* = 8.7 Hz, 2H, Ar-H), 4.11 – 4.01 (m, 8H, OCH_2CH_2), 1.89 – 1.74 (m, 8H, OCH_2CH_2), 1.58 – 1.44 (m, 8H, CH_2), 1.42 – 1.25 (m, 20H, CH_2), 0.94 – 0.87 (m, 12H, CH_3); ^{13}C NMR (126 MHz, $CDCl_3$) δ 165.05, 158.95 (C=O), 152.98, 150.64, 143.21, 143.10, 138.44, 138.23, 137.43, 133.65, 133.10, 132.92, 132.33, 131.64, 128.34, 128.28, 124.46, 124.21, 123.81, 122.30, 122.23, 121.72, 121.69, 114.97, 108.64 (BTBT-C + Ar-C), 73.58, 69.30, 68.16 (OCH_2), 31.81, 31.71, 31.54, 30.28, 29.36, 29.29, 29.26, 29.23, 26.06, 25.73, 25.69, 22.66, 22.65, 22.59 (CH_2), 14.08, 14.06, 14.00 (CH_3); HRMS (m/z): $[M]+Li^+$ calcd. for $C_{59}H_{72}O_6S_2Li$, 947.493; found 947.501.

2-[4-(3,4,5-Tri-n-hexyloxybenzoyloxy)phenyl]-7-(4-nonyloxyphenyl)-[1]benzothieno[3,2-b]benzothiophene (H9): H-OH (100 mg, 0.121 mmol), K_2CO_3 (200 mg, 1.447 mmol), TBAI (20 mg, 0.0541 mmol), 1-bromononane (75 mg, 0.362 mmol) and butanone (50 ml); yield 40 mg (0.0419 mmol, 35%); colorless solid; M = 955.36 g mol^{-1}; ^{1}H NMR (500 MHz, $CDCl_3$) δ 8.11 (dd, *J* = 22.7, 1.1 Hz, 2H, BTBT-H), 7.94 (dd, *J* = 12.1, 8.3 Hz, 2H, BTBT-H), 7.75 (d, *J* = 8.7 Hz, 2H, Ar-H), 7.69 (ddd, *J* = 16.7, 8.3, 1.6 Hz, 2H, BTBT-H), 7.62 (d, *J* = 8.8 Hz, 2H, Ar-H), 7.45 (s, 2H, Ar-H), 7.33 (d, *J* = 8.7 Hz, 2H, Ar-H), 7.02 (d, *J* = 8.8 Hz, 2H, Ar-H), 4.10 – 4.01 (m, 8H, OCH_2CH_2), 1.89 – 1.74 (m, 8H, OCH_2CH_2), 1.56 – 1.45 (m, 8H, CH_2), 1.40 – 1.27 (m, 22H, CH_2), 0.94

– 0.88 (m, 12H, CH_3); ^{13}C NMR (126 MHz, $CDCl_3$) δ 165.06, 158.96 (C=O), 152.98, 150.65, 143.22, 143.11, 138.45, 138.23, 137.43, 133.66, 133.11, 132.33, 131.65, 128.35, 128.29, 124.46, 124.22, 123.82, 122.31, 122.24, 121.74, 121.70, 114.97, 108.65 (BTBT-C + Ar-C), 73.59, 69.31, 68.17 (OCH_2), 31.87, 31.72, 31.54, 30.29, 29.54, 29.41, 29.30, 29.26, 26.06, 25.74, 25.69, 22.66, 22.60 (CH_2), 14.09, 14.06, 14.00 (CH_3); HRMS (m/z): $[M]+Li^+$ calcd. for $C_{60}H_{74}O_6S_2Li$, 961.508; found 961.513.

2-[4-(3,4,5-Tri-n-hexyloxybenzoyloxy)phenyl]-7-(4-decyloxyphenyl)-[1]benzothieno[3,2-b]benzothiophene (H10): H-OH (100 mg, 0.121 mmol), K_2CO_3 (200 mg, 1.447 mmol), TBAI (20 mg, 0.0541 mmol), 1-bromodecane (80 mg, 0.361 mmol) and butanone (50 ml); yield 33 mg (0.0340 mmol, 28%); colorless solid; M = 969.38 g mol^{-1}; ^1H NMR (500 MHz, $CDCl_3$) δ 8.11 (dd, *J* = 22.7, 0.9 Hz, 2H, BTBT-H), 7.93 (dd, *J* = 12.0, 8.2 Hz, 2H, BTBT-H), 7.75 (d, *J* = 8.6 Hz, 2H, Ar-H), 7.69 (ddd, *J* = 16.7, 8.3, 1.5 Hz, 2H, BTBT-H), 7.62 (d, *J* = 8.7 Hz, 2H, Ar-H), 7.45 (s, 2H, Ar-H), 7.33 (d, *J* = 8.6 Hz, 2H, Ar-H), 7.02 (d, *J* = 8.7 Hz, 2H, Ar-H), 4.11 – 4.00 (m, 8H, OCH_2CH_2), 1.89 – 1.75 (m, 8H, OCH_2CH_2), 1.57 – 1.45 (m, 8H, CH_2), 1.41 – 1.23 (m, 24H, CH_2), 0.95 – 0.87 (m, 12H, CH_3); ^{13}C NMR (126 MHz, $CDCl_3$) δ 165.05, 158.95 (C=O), 152.98, 150.64, 143.21, 143.10, 138.44, 138.22, 137.42, 133.65, 133.10, 132.92, 132.32, 131.64, 128.34, 128.28, 124.45, 124.21, 123.81, 122.30, 122.23, 121.73, 121.69, 114.97, 108.64 (BTBT-C + Ar-C), 73.58, 69.30, 68.16 (OCH_2), 31.89, 31.71, 31.54, 30.28, 29.58, 29.55, 29.40, 29.31, 29.29, 29.26, 26.06, 25.74, 25.69, 22.66, 22.60 (CH_2), 14.09, 14.06, 14.00 (CH_3); HRMS (m/z): $[M]+Li^+$ calcd. for $C_{61}H_{76}O_6S_2Li$, 975.524; found 975.531.

2-[4-(3,4,5-Tri-n-hexyloxybenzoyloxy)phenyl]-7-(4-undecyloxyphenyl)-[1]benzothieno[3,2-b]benzothiophene (H11): H-OH (100 mg, 0.12 mmol), K_2CO_3 (200 mg, 1.45 mmol), TBAI (20 mg, 0.054 mmol), 1-bromoundecane (85 mg, 0.36 mmol) and butanone (50 ml); yield 45 mg (0.046 mmol, 38%); colorless solid; M = 983.41 g $mol^{-1}$$^1H$ NMR (400 MHz, $CDCl_3$) δ 8.12 (dd, *J* = 18.1, 1.2 Hz, 2H, BTBT-H), 7.94 (dd, *J* = 9.4, 8.6 Hz, 2H, BTBT-H), 7.75 (d, *J* = 8.6 Hz, 2H, Ar-H), 7.69 (ddd, *J* = 13.3, 8.3, 1.6 Hz, 2H, BTBT-H), 7.62 (d, *J* = 8.7 Hz, 2H, Ar-H), 7.45 (s, 2H, Ar-H), 7.33 (d, *J* = 8.6 Hz, 2H, Ar-H), 7.02 (d, *J* = 8.7 Hz, 2H, Ar-H), 4.10 – 4.00 (m, 8H, OCH_2CH_2), 1.89 – 1.74 (m, 8H, OCH_2CH_2), 1.59 – 1.44 (m, 8H, CH_2), 1.41 – 1.24 (m, 26H, CH_2), 0.96 – 0.85

(m, 12H, CH_3); ^{13}C NMR (101 MHz, $CDCl_3$) δ 165.05, 158.96 (C=O), 152.98, 150.64, 143.21, 143.10, 138.23, 137.43, 133.66, 133.10, 132.92, 131.64, 128.34, 128.28, 124.46, 124.21, 123.81, 122.30, 122.23, 121.74, 121.73, 121.70, 114.97, 108.64 (BTBT-C + Ar-C), 73.58, 69.30, 68.16 (OCH_2), 31.90, 31.71, 31.54, 30.28, 29.61, 29.60, 29.57, 29.40, 29.32, 29.29, 29.26, 26.05, 25.74, 25.69, 22.67, 22.60 (CH_2), 14.09, 14.06, 14.00 (CH_3); HRMS (m/z): $[M]+Li^+$ calcd. for $C_{62}H_{78}O_6S_2Li$, 989.540; found 989.542.

2-[4-(3,4,5-Tri-n-hexyloxybenzoyloxy)phenyl]-7-(4-dodecyloxyphenyl)-[1]benzothieno[3,2-b]benzothiophene (H12): H-OH (100 mg, 0.12 mmol), K_2CO_3 (200 mg, 1.45 mmol), TBAI (20 mg, 0.054 mmol), 1-bromododecane (90 mg, 0.36 mmol) and butanone (50 ml); yield 38 mg (0.038 mmol, 31%); colorless solid; M = 997.44 g mol^{-1}; ^1H NMR (500 MHz, $CDCl_3$) δ 8.12 (dd, *J* = 22.7, 1.4 Hz, 2H, BTBT-H), 7.94 (dd, *J* = 12.1, 8.3 Hz, 2H, BTBT-H), 7.75 (d, *J* = 8.6 Hz, 2H, Ar-H), 7.69 (ddd, *J* = 16.7, 8.2, 1.5 Hz, 2H, BTBT-H), 7.62 (d, *J* = 8.6 Hz, 2H, Ar-H), 7.45 (s, 2H, Ar-H), 7.33 (d, *J* = 8.5 Hz, 2H, Ar-H), 7.02 (d, *J* = 8.7 Hz, 2H, Ar-H), 4.10 – 4.01 (m, 8H, OCH_2CH_2), 1.88 – 1.75 (m, 8H, OCH_2CH_2), 1.54 – 1.46 (m, 8H, CH_2), 1.40 – 1.25 (m, 28H, CH_2), 0.94 – 0.87 (m, 12H, CH_3); ^{13}C NMR (101 MHz, $CDCl_3$) δ 165.05, 158.96 (C=O), 152.98, 150.65, 143.21, 143.11, 143.10, 138.45, 138.23, 137.90, 137.85, 137.43, 133.66, 133.25, 132.92, 132.48, 132.33, 132.09, 129.56, 128.34, 128.29, 124.52, 124.46, 124.21, 123.81, 122.31, 122.24, 121.74, 121.72, 121.70, 114.97, 108.64 (BTBT-C + Ar-C), 73.58, 69.30, 68.17 (OCH_2), 31.91, 31.71, 31.54, 30.28, 29.65, 29.62, 29.59, 29.40, 29.33, 29.29, 29.26, 26.06, 25.74, 25.69, 22.66, 22.60 (CH_2), 14.10, 14.06, 14.00 (CH_3); HRMS (m/z): $[M]+Li^+$ calcd. for $C_{63}H_{80}O_6S_2Li$, 1003.555; found 1003.565.

3.2 Synthesis of compounds BB7-BB11

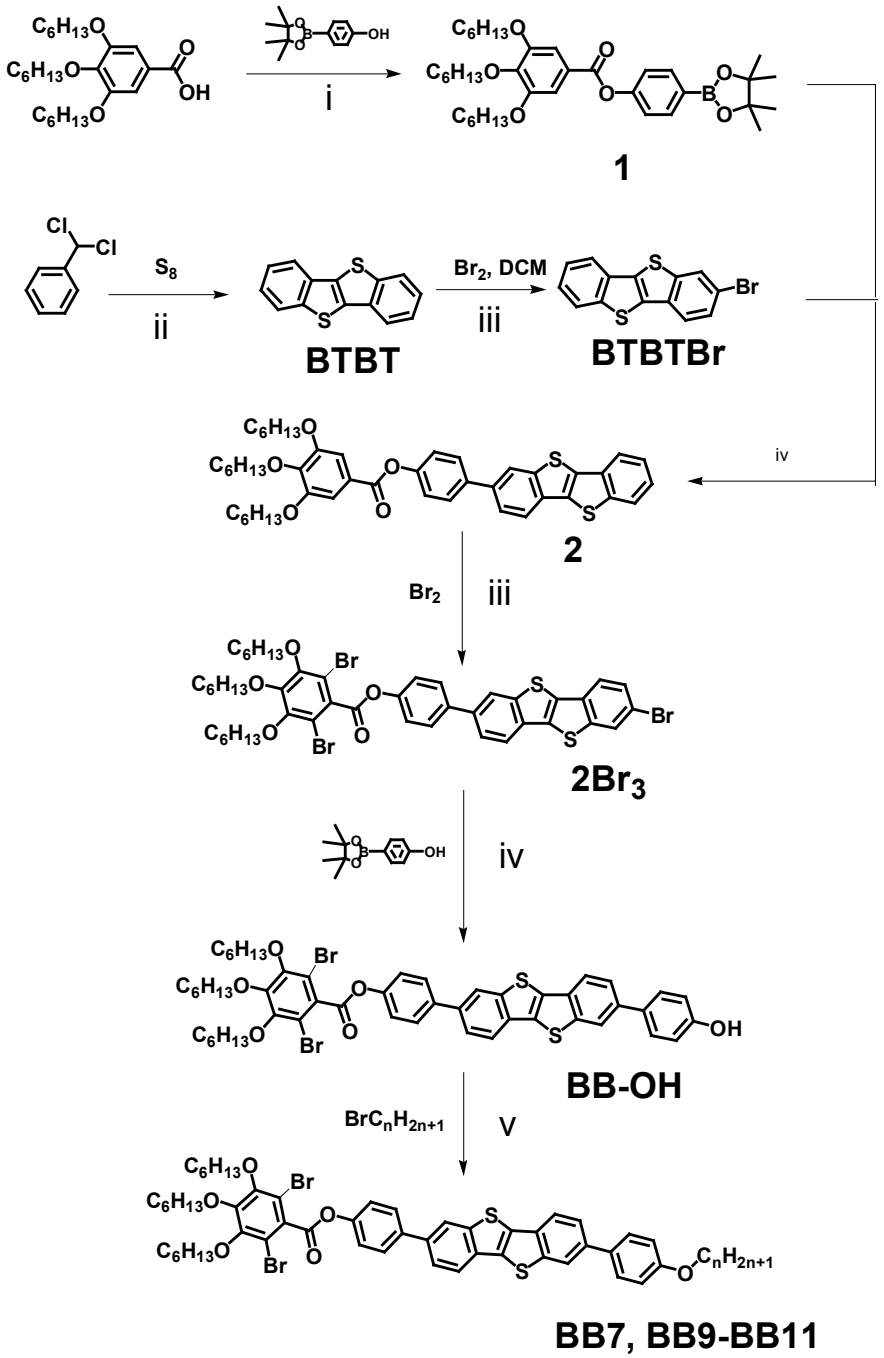

Scheme S3. Synthesis of compounds **BB7-BB11**. Reagents and conditions: (i) $SOCl_2$, dry pyridine, RT; (ii) 260 °C; (iii) DCM, RT; (iv) THF, sat. $NaHCO_3$ solution, $[Pd(PPh_3)_4]$, reflux; (v) dry 2-butanone, K_2CO_3; TBAI; reflux.

3.2.1 Intermediates

2-[4-(3,4,5-Tri-n-hexyloxybenzoyloxy)phenyl]-[1]benzothieno[3,2-b]benzothiophene (2) was prepared according to previously reported procedures [S8]

2-[4-(2,6-Dibromo-3,4,5-tri-n-hexyloxybenzoyloxy)phenyl]-7-bromo-[1]benzothieno[3,2-b]benzothiophene (2Br$_3$): The same procedure for **BTBT-Br** was used. **2** (1.20 g, 1.63 mmol), bromine (0.910 g, 5.71 mmol), DCM (60 ml), reaction time 72 h, RT, column chromatography (eluent: $CHCl_3$/n-hexane 2/1); yield 1.00 g (1.027 mmol, 63 %); colorless gel; ^{1}H NMR (500 MHz, $CDCl_3$) δ 8.08 (dd, *J* = 17.3, 1.6 Hz, 2H, BTBT-H), 8.04 (d, *J* = 1.4 Hz, 1H, BTBT-H), 7.86 (d, *J* = 1.4 Hz, 1H, BTBT-H), 7.74 – 7.70 (m, 3H, BTBT-H + Ar-H), 7.60 – 7.57 (m, 1H, BTBT-H), 7.46 (d, *J* = 8.7 Hz, 2H, Ar-H), 4.10 – 4.04 (m, 6H, OCH_2CH_2), 1.87 – 1.75 (m, 6H, OCH_2CH_2), 1.58 – 1.45 (m, 6H, CH_2), 1.41 – 1.20 (m, 12H, CH_2), 0.97 – 0.85 (m, 9H, CH_3).

2-[4-(2,6-Dibromo-3,4,5-tri-n-hexyloxybenzoyloxy)phenyl]-7-(4-hydroxyphenyl)-[1]benzothieno[3,2-b]benzothiophene (BB-OH): The same procedure for 2Br was used. 2Br3 (1.00 g, 1.027 mmol), 4-hydroxyphenylboronic acid pinacol ester (0.24 g, 1.10 mmol), THF (100 ml) and saturated NaHCO3 solution (50 ml), column chromatography (eluent: CHCl3/MeOH 19/1); yield 0.67 g (0.679 mmol, 66 %); colorless solid; heating: Cr 210 Iso (°C); cooling: Iso 205 SmA 190 Cr (°C); 1H NMR (400 MHz, CDCl3) δ 8.09 (dd, J = 20.1, 1.1 Hz, 2H, BTBT-H), 7.93 (dd, J = 10.4, 8.2 Hz, 2H, BTBT-H), 7.75 (d, J = 8.7 Hz, 2H, Ar-H), 7.67 (ddd, J = 16.0, 8.3, 1.6 Hz, 2H, BTBT-H), 7.58 (d, J = 8.7 Hz, 2H, Ar-H), 7.46 (d, J = 8.7 Hz, 2H, Ar-H), 6.94 (d, J = 8.7 Hz, 2H, Ar-H), 4.84 (s, 1H, Ar-OH), 4.07 (t, J = 6.6 Hz, 6H, OCH2CH2), 1.88 – 1.74 (m, 6H, OCH2CH2), 1.57 – 1.45 (m, 6H, CH2), 1.41 – 1.33 (m, 12H, CH2), 0.93 (t, J = 7.0 Hz, 9H, CH3).

3.2.2 Compounds BB7 and BB9 – BB12

2-[4-(2,6-Dibromo-3,4,5-tri-n-hexyloxybenzoyloxy)phenyl]-7-(4-heptyloxyphenyl)-[1]benzothieno[3,2-b]benzothiophene (BB7): BB-OH (120 mg, 0.122 mmol), K_2CO_3 (200 mg, 1.447 mmol), TBAI (20 mg, 0.0541 mmol), 1-bromoheptane (65 mg, 0.365 mmol) and butanone

(50 ml); yield 72 mg (0.066 mmol, 55%); colorless solid; M =1085.09 g mol^{-1}; ^{1}H NMR (400 MHz, $CDCl_3$) δ 8.11 (dd, *J* = 11.8, 1.2 Hz, 2H, BTBT-H), 7.94 (dd, *J* = 9.0, 8.5 Hz, 2H, BTBT-H), 7.76 (d, *J* = 8.7 Hz, 2H, Ar-H), 7.68 (ddd, *J* = 8.4, 6.8, 1.6 Hz, 2H, BTBT-H), 7.62 (d, *J* = 8.8 Hz, 2H, Ar-H), 7.46 (d, *J* = 8.6 Hz, 2H, Ar-H), 7.02 (d, *J* = 8.8 Hz, 2H, Ar-H), 4.10 – 4.01 (m, 8H, OCH_2CH_2), 1.88 – 1.74 (m, 8H, OCH_2CH_2), 1.56 – 1.43 (m, 8H, CH_2), 1.42 – 1.30 (m, 18H, CH_2), 0.96 – 0.88 (m, 12H, CH_3); ^{13}C NMR (101 MHz, $CDCl_3$) δ 164.41, 158.95 (C=O), 150.96, 148.57, 143.22, 143.10, 139.18, 138.24, 133.71, 132.92, 132.40, 132.37, 131.63, 128.50, 128.29, 124.51, 124.21, 122.36, 121.94, 121.74, 121.71, 114.97, 109.96 (BTBT-C + Ar-C), 74.62, 74.45, 68.16 (OCH_2), 31.78, 31.61, 30.14, 29.29, 29.07, 26.02, 25.64, 25.63, 22.60 (CH_2), 14.07, 14.03, 14.00 (CH_3); HRMS (m/z): [M]+Li^+ calcd. for $C_{58}H_{68}Br_2O_6S_2Li$, 1089.298; found 1089.309.

2-[4-(2,6-Dibromo-3,4,5-tri-n-hexyloxybenzoyloxy)phenyl]-7-(4-nonyloxyphenyl)-[1]benzothieno[3,2-b]benzothiophene (BB9): BB-OH (120 mg, 0.122 mmol), K_2CO_3 (200 mg, 1.447 mmol), TBAI (20 mg, 0.0541 mmol), 1-bromononane (75 mg, 0.365 mmol) and butanone (50 ml); yield 48 mg (0.0431 mmol, 35%); colorless solid; M = 1113.15 g mol^{-1};^{1}H NMR (400 MHz, $CDCl_3$) δ 8.11 (dd, *J* = 11.8, 1.4 Hz, 2H, BTBT-H), 7.94 (dd, *J* = 9.0, 8.6 Hz, 2H, BTBT-H), 7.76 (d, *J* = 8.6 Hz, 2H, Ar-H), 7.68 (ddd, *J* = 8.4, 7.0, 1.5 Hz, 2H, BTBT-H), 7.62 (d, *J* = 8.6 Hz, 2H, Ar-H), 7.46 (d, *J* = 8.6 Hz, 2H, Ar-H), 7.02 (d, *J* = 8.7 Hz, 2H, Ar-H), 4.10 – 4.01 (m, 8H, OCH_2CH_2), 1.88 – 1.74 (m, 8H, OCH_2CH_2), 1.56 – 1.44 (m, 8H, CH_2), 1.41 – 1.26 (m, 22H, CH_2), 0.96 – 0.87 (m, 12H, CH_3);^{13}C NMR (101 MHz, $CDCl_3$) δ 164.42, 159.95 (C=O), 150.96, 150.96, 150.07, 148.57, 143.10, 139.18, 138.25, 137.35, 133.09, 132.92, 132.40, 131.63, 128.50, 128.29, 124.51, 124.22, 122.36, 121.94, 121.75, 121.71, 121.70, 114.97, 109.96 (BTBT-C + Ar-C), 74.61, 74.45, 68.16 (OCH_2), 31.87, 31.61, 30.14, 29.53, 29.40, 29.29, 29.25, 26.05, 25.64, 25.63, 22.66, 22.60 (CH_2), 14.09, 14.03, 14.00 (CH_3); HRMS (m/z): [M]+Li^+ calcd. for $C_{60}H_{72}Br_2O_6S_2Li$, 1117.329; found 1117.325.

2-[4-(2,6-Dibromo-3,4,5-tri-n-hexyloxybenzoyloxy)phenyl]-7-(4-decyloxyphenyl)-[1]benzothieno[3,2-b]benzothiophene (BB10): BB-OH (120 mg, 0.122 mmol), K_2CO_3 (200 mg, 1.447 mmol), TBAI (20 mg, 0.0541 mmol), 1-bromodecane (80 mg, 0.365 mmol) and butanone (50 ml); yield 35 mg (0.0311 mmol, 26%); colorless solid; M = 1127.17 g mol^{-1}; ^{1}H NMR (400

MHz, $CDCl_3$) δ 8.11 (dd, *J* = 11.8, 1.1 Hz, 2H, BTBT-H), 7.94 (dd, *J* = 9.0, 8.5 Hz, 2H, BTBT-H), 7.76 (d, *J* = 8.7 Hz, 2H, Ar-H), 7.68 (ddd, *J* = 8.4, 6.9, 1.6 Hz, 2H, BTBT-H), 7.62 (d, *J* = 8.8 Hz, 2H, Ar-H), 7.46 (d, *J* = 8.6 Hz, 2H, Ar-H), 7.02 (d, *J* = 8.8 Hz, 2H, Ar-H), 4.09 – 4.00 (m, 8H, OCH_2CH_2), 1.88 – 1.74 (m, 8H, OCH_2CH_2), 1.57 – 1.44 (m, 8H, CH_2), 1.42 – 1.24 (m, 24H, CH_2), 0.96 – 0.87 (m, 12H, CH_3); ^{13}C NMR (126 MHz, $CDCl_3$) δ 164.41, 158.95 (C=O), 150.96, 150.07, 148.57, 143.22, 143.10, 139.18, 138.24, 137.35, 133.71, 133.09, 132.92, 132.40, 132.37, 131.63, 128.50, 128.29, 124.51, 124.21, 122.36, 121.94, 121.75, 121.71, 114.97, 109.96 (BTBT-C + Ar-C), 74.62, 74.45, 68.16 (OCH_2), 31.88, 31.61, 30.14, 29.58, 29.55, 29.40, 29.31, 29.29, 26.05, 25.64, 25.63, 22.66, 22.60 (CH_2), 14.09, 14.03, 14.00 (CH_3); HRMS (m/z): $[M]+Li^+$ calcd. for $C_{61}H_{74}Br_2O_6S_2Li$, 1131.345; found 1131.352.

2-[4-(2,6-Dibromo-3,4,5-tri-n-hexyloxybenzoyloxy)phenyl]-7-(4-undecyloxyphenyl)-[1]benzothieno[3,2-b]benzothiophene (BB11): BB-OH (120 mg, 0.122 mmol), K_2CO_3 (200 mg, 1.447 mmol), TBAI (20 mg, 0.0541 mmol), 1-bromoundecane (85 mg, 0.365 mmol) and butanone (50 ml); yield 55 mg (0.0482 mmol, 40%); colorless solid; M = 1141.20 g mol^{-1}; ^1H NMR (400 MHz, $CDCl_3$) δ 8.11 (dd, *J* = 11.8, 1.1 Hz, 2H, BTBT-H), 7.94 (dd, *J* = 9.1, 8.5 Hz, 2H, BTBT-H), 7.76 (d, *J* = 8.5 Hz, 2H, Ar-H), 7.69 (ddd, *J* = 8.3, 6.9, 1.3 Hz, 2H, BTBT-H), 7.62 (d, *J* = 8.7 Hz, 2H, Ar-H), 7.46 (d, *J* = 8.5 Hz, 2H, Ar-H), 7.02 (d, *J* = 8.7 Hz, 2H, Ar-H), 4.09 – 4.01 (m, 8H, OCH_2CH_2), 1.88 – 1.74 (m, 8H, OCH_2CH_2), 1.56 – 1.45 (m, 8H, CH_2), 1.41 – 1.25 (m, 26H, CH_2), 0.95 – 0.87 (m, 12H, CH_3); ^{13}C NMR (101 MHz, $CDCl_3$) δ 158.95 (C=O), 150.96, 148.57, 139.18, 137.48, 136.58, 128.50, 128.29, 125.88, 124.51, 124.22, 122.37, 121.94, 121.75, 121.71, 114.97 (BTBT-C + Ar-C), 74.62, 74.45, 68.16 (OCH_2), 31.89, 31.60, 30.14, 29.60, 29.59, 29.57, 29.40, 29.32, 26.05, 25.64, 25.63, 24.72, 22.67, 22.60 (CH_2), 14.09, 14.02, 14.00 (CH_3); HRMS (m/z): $[M]+Li^+$ calcd. for $C_{62}H_{76}Br_2O_6S_2Li$, 1145.361; found 1145.367.

3.3 Synthesis of BB8

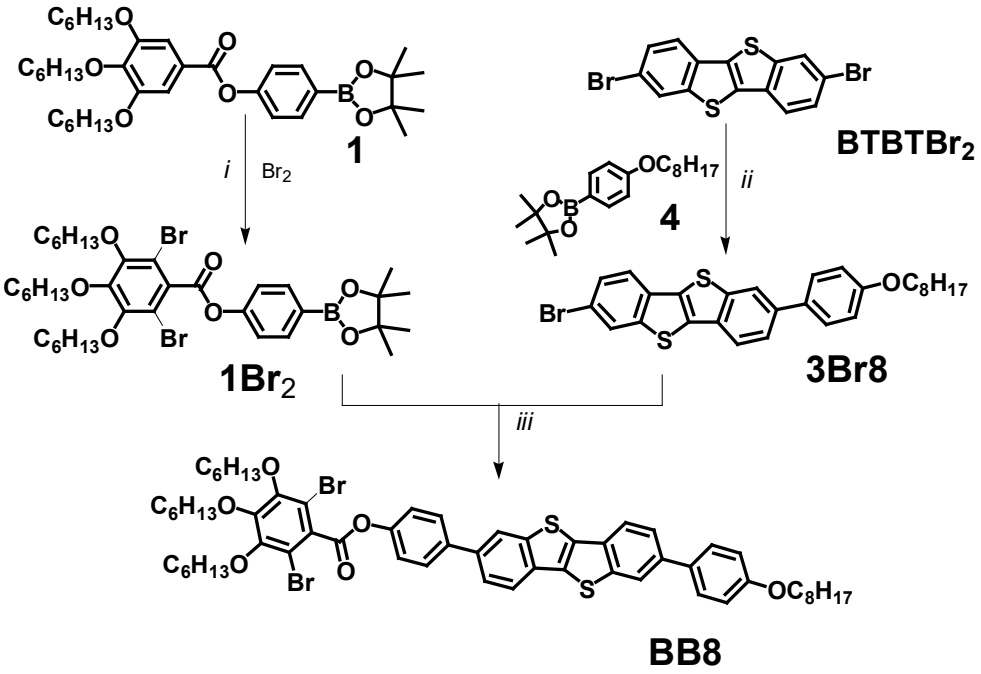

Scheme S4. Synthesis of compounds **BB8**. Reagents and conditions: (i) 2.2 eq. Br_2, DCM, RT (ii) 1.33 eq. **BTBT-Br$_2$**, THF, Toluene, sat. $NaHCO_3$ solution, [$Pd(PPh_3)_4$], reflux (iii) THF, sat. $NaHCO_3$ solution, [$Pd(PPh_3)_4$], reflux

3.3.1 Intermediates

4-(2,6-Dibromo-3,4,5-tri-n-hexyloxybenzoyloxy)phenylboronic acid pinacol ester (1Br$_2$): The same procedure for **BTBTBr** was used. **1** (1.00 g, 1.601 mmol), bromine 2.2 eq. (0.56 g, 3.522 mmol), DCM (60 ml), reaction time 72 h, RT, column chromatography (n-hexane/$CHCl_3$); yield: 0.62 g (0.792 mmol, 49%); colorless liquid; ^{1}H NMR (500 MHz, $CDCl_3$) δ 7.89 (d, *J* = 8.5 Hz, 2H, Ar-H), 7.32 (d, *J* = 8.5 Hz, 2H, Ar-H), 4.07 – 4.02 (m, 6H, OCH_2CH_2), 1.86 – 1.73 (m, 6H, OCH_2CH_2), 1.53 – 1.42 (m, 6H, CH_2), 1.39 – 1.31 (m, 24H, CH_2 + CH_3), 0.92 (t, *J* = 7.1 Hz, 9H, CH_3).

4-Octyloxyphenylboronic acid pinacol ester (4): The same procedure for **H8-H12** was used.4-Hydroxyphenylboronic acid pinacol ester (3.00 g, 13.63 mmol), K_2CO_3 (5.65 g, 40.89 mmol), TBAI (50 mg, 0.135 mmol), 1-bromooctane (2.90 g, 14.99 mmol), butanone (100 ml); yield: 2.1

g (6.32 mmol, 46%); colorless liquid; ^{1}H NMR (500 MHz, $CDCl_3$) δ 7.73 (d, *J* = 8.7 Hz, 2H, Ar-H), 6.88 (d, *J* = 8.7 Hz, 2H, Ar-H), 3.97 (t, *J* = 6.6 Hz, 2H, OCH_2CH_2), 1.81 – 1.74 (m, 2H, OCH_2CH_2), 1.48 – 1.40 (m, 2H, CH_2), 1.36 – 1.25 (m, 20H, CH_2 + CH_3), 0.89 (t, *J* = 7.0 Hz, 3H, CH_3).

2-Bromo-7-(4-octyloxyphenyl)-[1]benzothieno[3,2-b]benzothiophene (3Br8): The same procedure for **2Br** was used. **4** (1.00 g, 3.01 mmol), **BTBTBr2** (1.59 g, 4.00 mmol), THF (50 ml), toluene (100 ml), saturated $NaHCO_3$ solution (70 ml), [$Pd(PPh_3)_4$] (0.1 g, 0.0865 mmol) yield: 0.54 g (1.03 mmol, 34 %); colorless solid; heating: Cr 105 SmA 210 Iso (°C), cooling: Iso 208 SmA 88 Cr (°C); ^{1}H NMR (400 MHz, $CDCl_3$) δ 8.11 – 8.04 (m, 2H, 2H, BTBT-H), 7.96 – 7.81 (m, 2H, BTBT-H), 7.75 – 7.46 (m, 4H, Ar-H + BTBT-H), 7.03 – 6.98 (m, 2H, Ar-H), 4.08 (t, *J* = 6.5 Hz, 2H, OCH_2CH_2), 1.85 (qd, *J* = 14.0, 6.6 Hz, 2H, OCH_2CH_2), 1.56 – 1.43 (m, 2H, CH_2), 1.43 – 1.25 (m, 8H, CH_2), 0.90 (t, *J* = 6.7 Hz, 3H, CH_3).

3.3.2 Compound BB8

2-[4-(2,6-Dibromo-3,4,5-tri-n-hexyloxybenzoyloxy)phenyl]-7-(4-octyloxyphenyl)-[1]benzothieno[3,2-b]benzothiophene (BB8): The same procedure for **2Br** was used: **1Br$_2$** (0.55 g, 0.700 mmol), **3Br8** (0.54 g, 1.03 mmol), THF (50 ml), saturated $NaHCO_3$ solution (30 ml), [$Pd(PPh_3)_4$] (0.03 g, 0.0260 mmol) yield: 75 mg (0.0682 mmol, 10 %); colorless solid; M = 1099.12 g mol^{-1}; ^{1}H NMR (500 MHz, $CDCl_3$) δ 8.11 (dd, *J* = 14.7, 0.8 Hz, 2H, BTBT-H), 7.94 (dd, *J* = 11.5, 8.4 Hz, 2H, BTBT-H), 7.76 (d, *J* = 8.6 Hz, 2H, Ar-H), 7.69 (ddd, *J* = 9.2, 8.2, 1.2 Hz, 2H, BTBT-H), 7.62 (d, *J* = 8.5 Hz, 2H, Ar-H), 7.46 (d, *J* = 8.5 Hz, 2H, Ar-H), 7.02 (d, *J* = 8.7 Hz, 2H, Ar-H), 4.10 – 4.00 (m, 8H, OCH_2CH_2), 1.88 – 1.74 (m, 8H, OCH_2CH_2), 1.61 – 1.45 (s, 8H, CH_2), 1.41 – 1.23 (m, 20H, CH_2), 0.95 – 0.86 (m, 12H, CH_3); ^{13}C NMR (126 MHz, $CDCl_3$) δ 158.95 (C=O), 150.96, 150.07, 148.57, 143.10, 139.18, 138.25, 137.36, 128.50, 128.29, 122.37, 121.94, 121.75, 121.72, 114.97 (BTBT-C + Ar-C), 74.62, 74.45 (OCH_2), 31.81, 31.60, 30.92, 30.14, 29.67, 29.36, 29.29, 29.23, 26.06, 25.64, 25.63, 22.65, 22.60 (CH_2), 14.08, 14.02, 14.00 (CH_3); HRMS (m/z): [M]+Li^+ calcd. for $C_{59}H_{70}Br_2O_6S_2Li$, 1103.314; found 1103.317.

3.4 Representative NMR and HRMS spectra

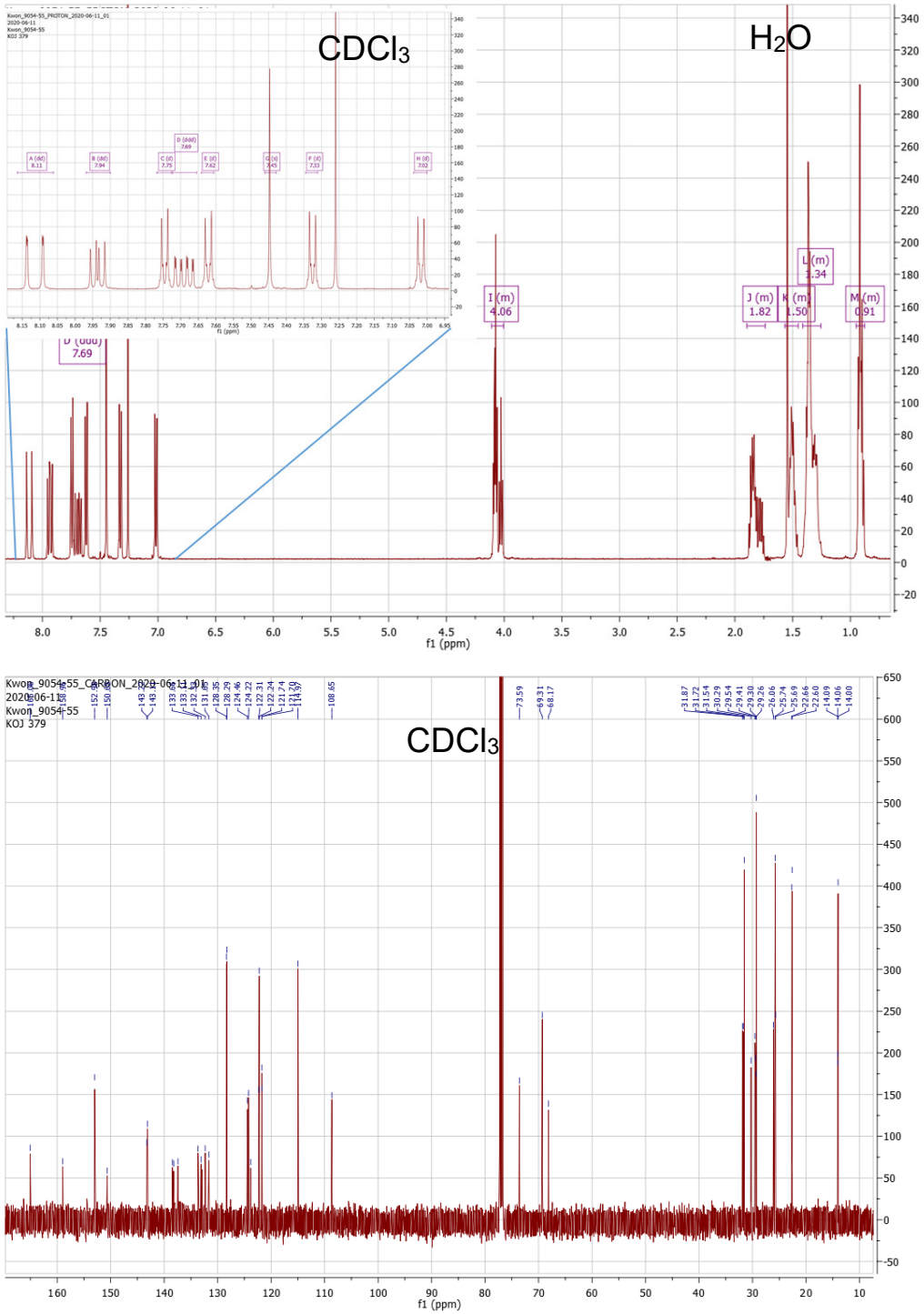

Figure S15. ^{1}H- and ^{13}C-NMR of compound **H9**. The spectra were measured at 27 °C, with the frequencies 500 MHz (^{1}H) and 126 MHz (^{13}C) in $CDCl_3$ as solvent.

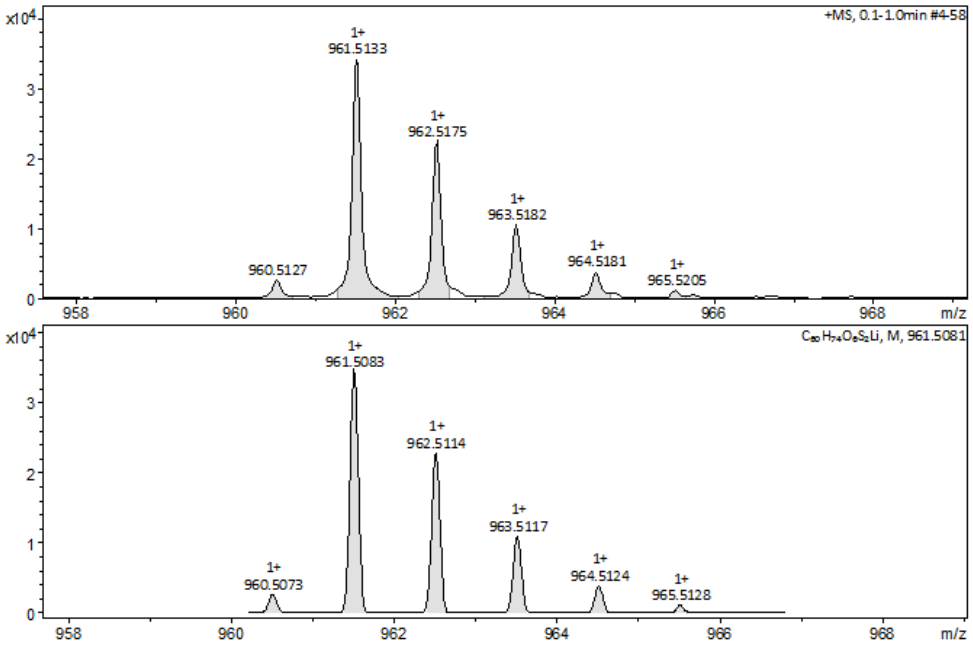

Figure S16. HRMS spectra for **H9.**

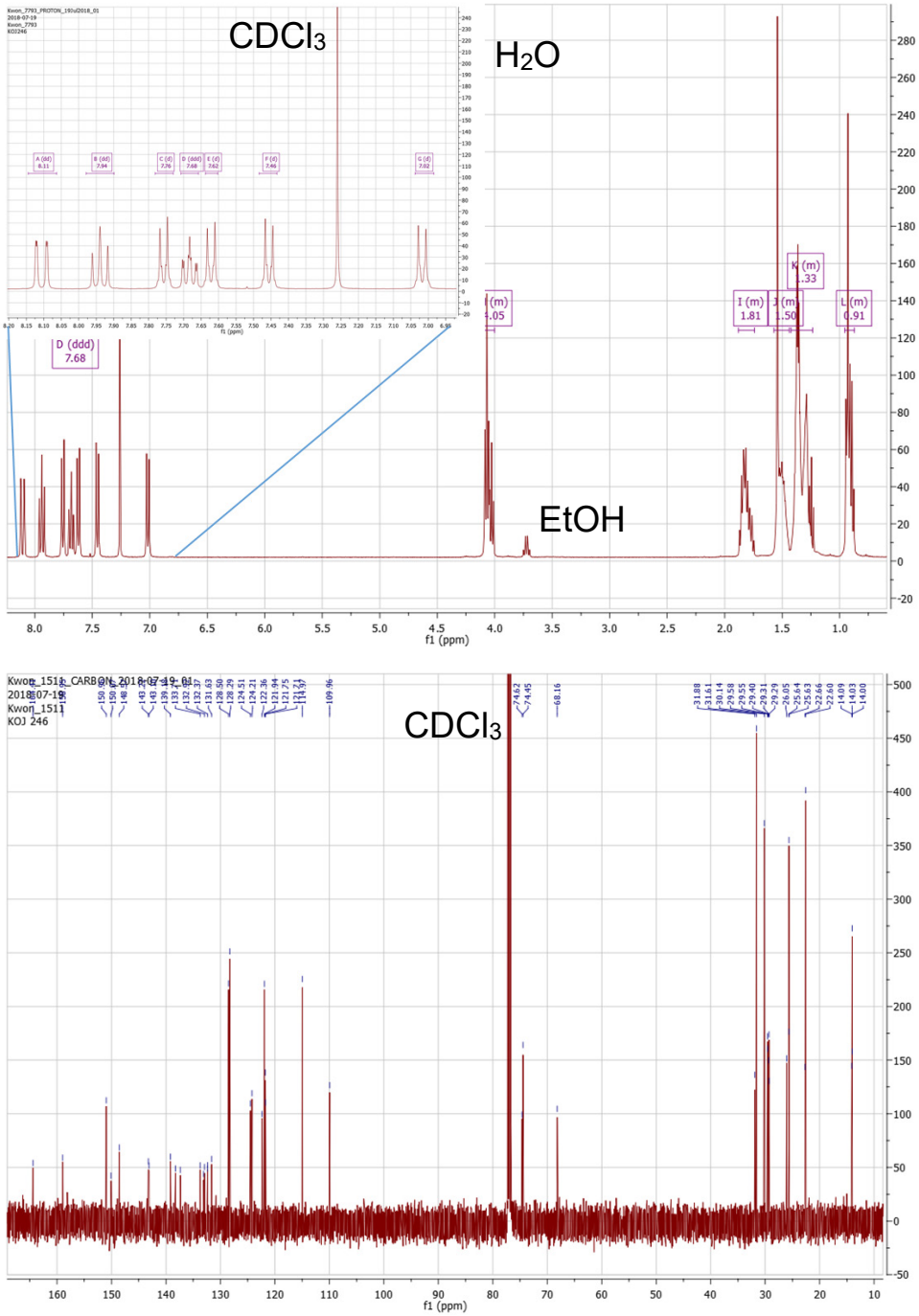

Figure S17. ^{1}H- and ^{13}C-NMR of compound **BB10**. The spectra were measured at 27 °C, with the frequencies 400 MHz (^{1}H) and 126 MHz (^{13}C) in $CDCl_3$ as solvent.

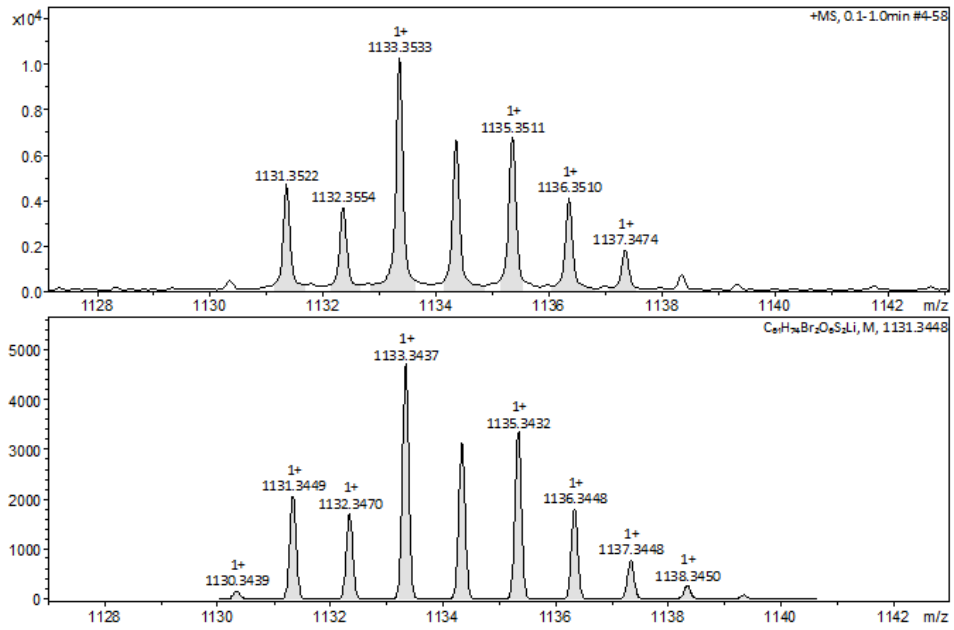

Figure S18. HRMS spectra for **BB10.**

4. References

S1 X. Zeng, G. Ungar, J. Mater. Chem. C, **2020**, 8, 5389.

S2 A. Immirzi and B. Perini, *Acta Cryst.* A **1977**, 33, 216.

S3 C. Dressel, T. Reppe, S. Poppe, M. Prehm, H. Lu, X. Zeng, G. Ungar, C. Tschierske, *Adv. Funct. Mater.* **2020**, 202004353

S4 V. A. Piunova, G. M. Miyake, C. S. Daeffler, R. A. Weitekamp, R. H. Grubbs, J. Am. Chem. Soc. **2013**, 135, 15609.

S5 C. Dressel, F. Liu, M. Prehm, X. Zeng, G. Ungar, C. Tschierske, Angew. Int. Ed. **2014**, 53, 13115.

S6 A. Sanzone, S. Mattiello, G. M. Garavaglia, A. M. Calascibetta, C. Ceriani, M. Sassi, & L. Beverina; Green Chem., 2019,21, 4400-4405

S7 N. Miyaura, A. Suzuki, Suzuki coupling reaction J. Chem. Soc. Chem. Commun. **1979**,19, 866.

S8 O. Kwon, X. Cai, W. Qu, F. Liu, J. Szydłowska, E. Gorecka, M. J. Han, D. K. Yoon S. Poppe and C. Tschierske, *Adv. Mater*, DOI: 10.1002/adfm.202102271.